The Criteria For The Number Of Bound States With $l = 0$ For A Non-Relativistic Single-Particle Potential

by

Anas Othman

A thesis submitted in partial fulfillment of the requirements for the degree of

Master of Science

Department of Physics

University of Alberta

Abstract

We have studied some criteria for bound state energies in the non-relativistic regime by using the $3D$ Schrödinger equation. With these criteria, we have examined: the number of bound states, the critical conditions, eigenvalues, and infinite versus finite number of eigenvalues, and the fixed number expression, which determines the number of bound states. We have studied these criteria by solving the Schrödinger equation in $3D$ for $l = 0$ for many central potentials: the finite spherical potential, the spherical potential shell, the Yukawa potential, the cutoff and regular triangular potential, the Woods-Saxon potential, the regular and cutoff Coulomb potential, and the cutoff inverse square and cubic potentials. By a cutoff potential we mean just a potential cutoff near the origin by connecting a potential with the finite spherical potential. Then, we have used some estimating methods to compare these results with the exact results. The estimating methods are expressions that give the lower and upper limits of the number of bound state energies for a given potential. We have considered these accurate and recent expressions and we have compared them with the exact results.

Acknowledgements

First of all I would like to thank **My God** about every single thing. Then, I thank my supervisor **Prof. Frank Marsiglio** about all his helpful advices . Also, I would like to thank **Prof. Marc de Montigny** about all his cooperation. Also, I cannot forget **Prof. Faqir Khanna** about all his welcoming and advising me. Moreover, I like to thank every single one helped or advised me to finsh this thesis including my wife **Basma Shawsh** and my mother **Aish Al-Turk**. Also, many thanks to my university **Taibah university**. To conclude, to whom I have thanked this small acknowledgement is not sufficient to thank you.

Contents

List of Tables

List of Figures

List of Abbreviations

TISE	Time independent Schrödinger equation
SE	Schrödinger equation
DE	Differential equation
NBSE	Number of bound state energies
FNE	Fixed number expression
3D	3-Dimensional
2D	2-Dimensional
1D	1-Dimensional

Chapter 1

Introduction

In classical mechanics, it is possible to determine the trajectory of a particle under the influence of a potential, and its energy can take on any physical value. However, this is not the case in quantum mechanics. We can only know the probability of finding the particle in a certain period of time and in a given volume. Also, the energies of bound states take on discrete values, a phenomenon known as energy quantization. The energy quantization started with an assumption by Max Planck in order to describe the black body radiation. Then, through Albert Einstein's concept of the photon in 1905, it came to be accepted that light energy is quantized and that light exhibits wave-particle duality. In 1924, Louis de Broglie extended the concept of wave-particle duality to matter. Three years later, this hypothesis was verified experimentally by the Davisson-Germer experiment through electron diffraction [1]. In 1925, Werner Heisenberg introduced quantum mechanics through the matrix formulation. Meanwhile, in 1926, Erwin Schrödinger developed an alternative but equivalent formulation of quantum mechanics through a matter wave function described by an equation that bears his name. However, one of the outcomes of the Schrödinger equation is that the bound state energies are always quantized. Within the context of classical mechanics, the existence of bound states means that the particle is between two turning points [2].

Many analytical and numerical studies have been performed to solve the Schrödinger equation (SE) for finding the eigenvalues and eigenfunctions for various types of potentials. Moreover, some of these studies went beyond this point and investigated the criteria for bound state energies or eigenvalues of the Schrödinger equation. In this work, the criteria for bound states include, for example, the number of bound states, the minimum condition for a bound state to exist, the value of

their energies, etc. Between 1926 and 1950, physicists were interested in studying the interpretations of SE and the new phenomena that arise through quantum mechanics. Thereafter, physicists started to think about the general criteria for bound state energies for a given potential. The earliest studies concerning these questions were by Jost and Pais [3] and Bargmann [4]; in particular, they worked on predicting the number of bound states for a given potential.

In this thesis, we will study the criteria for bound state energies in the non-relativistic regime described by the Schrödinger equation. Our main interest is to know the number of bound state energies and other related quantities for a given potential in three dimensions (3D). For example, we would like to know whether the number of bound state energies is finite or infinite (Chapter4). Also, in this study we will describe the values of the bound state energies for some potentials and how they are described by the quantum numbers. Moreover, I will briefly describe potentials in $1D$ and $2D$ and their most important criteria for bound state energies. The central topic of this thesis are the cases in $3D$ with $l = 0$, where l is the azimuthal quantum number connected to the angular momentum. Furthermore, this study is limited by its focus on potentials which are attractive for their entire range.

Our main results of this study are as follows: the most accurate estimating method for determining the upper and lower limits for the number of bound state energies are the Brau and Calogero limits [5] [6], which are discussed in Ch.(3). Also, the best method for estimating the critical conditions is the expanded Schwinger bound [7]. Moreover, we solve the SE in $3D$ for many potentials and obtain the energy equation which allows us to find the eigenvalues explicitly (see Chapters3 and4). We introduce the idea of the fixed number expression (FNE) which is defined in Section1.1. We found this expression explicitly for the two-parameter potentials and implicitly for some of the three-parameter potentials in Chapter3.

1.1 One dimension

It is well known that for a given attractive potential in one dimension there is at least one bound state energy. In this section we are going to give a proof of the existence for at least one bound state energy; also, we will determine the upper and lower limits in terms of the number of bound states. To show this we will use the Rayleigh-Ritz variational principle which claims that the expectation value of the Hamiltonian for a trial wavefunction is always greater than or equal to the ground state

energy.

$$\langle\psi_{trial}|H|\psi_{trial}\rangle \geq \langle\psi_{GS}|H|\psi_{GS}\rangle = E_0, \tag{1.1}$$

where $|\psi_{trial}\rangle$ is the trial wavefunction and $|\psi_{GS}\rangle$ is the ground state wavefunction. For any potential that has a depth V_0 and a finite range R, we can predict the general behaviour of its ground state wavefunction from our experience with ground state wavefunctions which should be nodeless. Let us suppose that this trial wavefunction has a width parameter α:

$$\psi_{trial}(x) = \left(\frac{1}{2\pi\alpha}\right)^{1/4} \exp\left(\frac{-x^2}{4\alpha}\right). \tag{1.2}$$

The expectation value of the Hamiltonian can be written as the sum of the kinetic and potential energy terms

$$\langle H\rangle = \langle T\rangle + \langle V\rangle. \tag{1.3}$$

Then, the expectation value of the kinetic energy is

$$\langle T\rangle = -\frac{\hbar^2}{2m}\int_{-\infty}^{\infty} \psi^*_{trial}\frac{d^2\psi_{trial}}{dx^2}\,dx = \frac{\hbar^2}{8m\alpha}. \tag{1.4}$$

The expectation value of V can be written as

$$\langle V\rangle = \int_{-\infty}^{\infty} \psi_{trial}(x)^2 V(x)\,dx \approx \psi_{trial}(0)^2\int_{-\infty}^{\infty} V(x)\,dx \approx -\frac{V_0 R}{\sqrt{2\pi\alpha}}. \tag{1.5}$$

This calculation is carried out by assuming that $\alpha \gtrsim R$. Then, the expectation value of the Hamiltonian gives

$$\langle H\rangle = -\frac{V_0 R}{\sqrt{2\pi\alpha}} + \frac{\hbar^2}{8m\alpha}. \tag{1.6}$$

Let us minimize this expression in order to find α_{min}:

$$\alpha_{min} = \frac{\hbar^4}{8m^2R^2V_0^2}. \tag{1.7}$$

Then (1.6) reads:

$$\langle H\rangle_{min} = -\frac{mV_0^2R^2}{\pi\hbar^2} \geq E_0 \tag{1.8}$$

This equation implies that whatever the values of R and V_0 are, there exists at least one bound state energy, so we can conclude this calculation by saying that solving the Schrödinger equation in $1D$ for an attractive potential always gives at least one bound state energy. For a similar proof see [8], [9].

We now perform a simple calculation to obtain the number of bound state energies. Chadan et al. [10] determined the upper limit of the number of bound state energies in the $1D$ Schrödinger equation for a potential $V(x)$, with $U = 2m/\hbar^2$

$$N < 1 + U \int_{-\infty}^{\infty} |x| V^{-}(x)\, dx, \tag{1.9}$$

where N is the number of bound state energies, and $V^{-}(x)$ is the absolute value of the negative part of the potential. This limit determines whether a potential has an infinite or finite number of bound states. For example, a finite square potential well has this definition ($V_0 > 0$):

$$V(x) = \begin{cases} -V_0 & \text{if } 0 < x < X; \\ 0 & \text{elsewhere.} \end{cases} \tag{1.10}$$

Equation (1.9) then yields

$$N < 1 + \frac{U V_0 X^2}{2}. \tag{1.11}$$

Then, the finite square potential has a finite number of bound states which is always equal to or greater than 1. Moreover, from Eq.(1.11) we can define the *fixed number expression* for this potential:

$$\mathbf{G} = U V_0 X^2. \tag{1.12}$$

For more details about the upper and lower limits in the $1D$ SE see Refs. [5], [11], [12].

Definition 1. Fixed number expression (G)

For a given potential there exists an expression which will be a function of the potential's parameters, if this expression is fixed, the number of bound state energies (N) will be fixed as well, so if this expression is known, we can write $N = f(\mathbf{G})$.

1.2 Two dimensions

The two dimensional SE does not differ from the one-dimensional SE in terms of the existence of at least one bound state energy for any purely attractive potentials. Hereafter, we will follow the same approach for the proof as in the $1D$ problem; that is by utilizing the Rayleigh-Ritz variational principle. The following result is obtained in Ref. [8] (see also Ref. [13]). Let us define the trial wavefunction as:

$$\psi_{trial}(r) = \begin{cases} \frac{K}{\alpha}\left(1-\frac{r+R}{\alpha}\right)\ln\left(\frac{r+R}{\alpha}\right) & \text{if } r \leq \alpha - R; \\ 0 & \text{if } r > \alpha - R. \end{cases} \tag{1.13}$$

where K is of order unity, and it assumed that $\alpha \gg R$. Then, let us calculate the expectation value of the kinetic and potential energy, and we find:

$$\langle T\rangle = \frac{\hbar^2}{2m\alpha^2}\int_{R/\alpha}^{1}\left|\frac{d\psi_{trial}}{du}\right|^2(\alpha u - R)2\pi\alpha\, du \approx \frac{\pi\hbar^2K^2}{m\alpha^2}\ln(\alpha/R), \tag{1.14}$$

where $u = \frac{r+R}{\alpha}$, and

$$\langle V\rangle \approx -V_0\int_{R/\alpha}^{2R/\alpha}|\psi_{trial}|^2(\alpha u - R)2\pi\alpha\, du \approx -\pi V_0K^2\left[\frac{R}{\alpha}\ln(\alpha/R)\right]^2, \tag{1.15}$$

hence,

$$\langle H\rangle = -\pi V_0K^2\left[\frac{R}{\alpha}\ln(\alpha/R)\right]^2 + \frac{\pi\hbar^2K^2}{m\alpha^2}\ln(\alpha/R). \tag{1.16}$$

After minimizing $\langle H\rangle$ with respect to α, we find

$$\langle H\rangle_{min} \approx -\frac{\hbar^2}{mR^2}\exp\left(\frac{-2\hbar^2}{mR^2V_0}\right). \tag{1.17}$$

Since equation (1.17) is always negative, that indicates that all attractive potentials in the $2D$ Schrödinger equation have at least one bound energy.

Let us turn to the number of bound states for a given potential $V(r)$. Glaser et al. [14] found the lower limit for a two dimensional central potential, with $U = 2m/\hbar^2$, as

$$N > -\frac{U}{4}\int_0^\infty rV(r)\, dr. \tag{1.18}$$

This lower limit is able to determine many features of the criteria for number of bound states, for

instance, the fixed number expression, infinite or finite number of bound state energies ,etc. For more limits in the $2D$ SE see Refs. [11], [15], [16].

1.3 Three dimensions and the estimating methods

For the three-dimensional Schrödinger equation, the criteria for bound state energies behave differently than in one or two dimensions, since it is not necessary that a bound state energy exists for a given attractive potential. Instead, we have a **critical point**.

Definition 2. Critical point ($\mathbf{G_c}$)

For the $3D$ SE, for a given attractive potential with a finite number of bound state energies (NBSE), there exists a constant number $\mathbf{G_c}$ which, if we make $\mathbf{G}$ in Def.(1) higher than this number, will result in at least one bound state, and for $\mathbf{G}$ lower than this number there will be no bound state.

Let us give a brief history of the most important developments in estimating the number of bound state energies. While describing this history, we will represent the most important relations and equations in this field. Hereafter, we will focus on $l = 0$. The first calculations to estimate the number of bound state energies (NBSE) for a given potential $V(r)$ were carried out by Bargmann [4] and Schwinger [7] based on [3]. They used a functional of $V(r)$ to determine the upper limit of NBSE for central potentials.

$$N_l < \frac{U}{2l+1}\int_0^\infty rV^-(r)\,dr, \qquad U = \frac{2m}{\hbar^2}, \tag{1.19}$$

where $V^-(r)$ is the absolute value of the negative part of the potential, namely, $V^-(r) = -V(r)\theta[-V(r)]$, where θ is the usual step function, and r is the radius from the origin. This limit is the so-called Bargmann-Schwinger bound [11]. This was a powerful estimate for determining whether a potential has an infinite or finite NBSE. However, the upper limit of Eq.(1.19) yields poor results for strong potentials. If we defined $V(r)$ to be:

$$V(r) = g^2 v(r), \tag{1.20}$$

where $v(r)$ is assumed to be independent of g, and g is a positive quantity called coupling constant, then a strong potential in this context means $g \to \infty$, where the Bargmann-Schwinger bound fails.

In 1967, Calogero [17] proved that N_l grows proportionally to g in the case $g \to \infty$

$$N_l \sim g \quad \text{as} \quad g \to \infty. \tag{1.21}$$

Then, Chadan [18] has shown that

$$N_l \approx \frac{1}{\pi} \int_0^\infty [V^-(r)]^{1/2}\, dr \qquad \text{as} \quad g \to \infty. \tag{1.22}$$

All previous results described NBSE for a specific value of l; [1] however, Martin [19] found that the total number of bound states $\mathcal{N}$ is given by

$$\mathcal{N} \approx \frac{2}{3\pi} \int_0^\infty r^2 [V^-(r)]^{3/2}\, dr \quad \text{as} \quad g \to \infty. \tag{1.23}$$

The developments to find $\mathcal{N}$ continued, but here we wish to refocus on the $l = 0$ case which we will simply label as $N_0 = N$. Calogero [20] and Cohn [21] obtained separately the upper limit as $g \to \infty$.

$$N < \frac{2}{\pi} \int_0^\infty [V^-(r)]^{1/2}\, dr. \tag{1.24}$$

This result is only valid when $V(r)$ is repulsive nowhere, and $V(r)$ is a monotonically non-decreasing function, means $dV(r)/dr > 0$. Also, Calogero found the lower limit for the monotonic potentials

$$N_l > \frac{2}{\pi} \frac{\rho |V(\rho)|^{1/2}}{2l+1} - \frac{1}{2}, \tag{1.25}$$

with the radius ρ defined to be the solution of the equation:

$$\rho V(\rho) = (2l+1) \int_\rho^\infty \left(\frac{\rho}{r}\right)^{2l} V(r)\, dr. \tag{1.26}$$

The next interesting result is due to Glaser et al. [22] and reads

$$N_l < \frac{(2l+1)^{1-2p}(p-1)^{p-1}\Gamma(2p)}{p^p \Gamma^2(p)} \int_0^\infty \frac{dr}{r} [r^2 V^-(r)]^p, \tag{1.27}$$

with the restriction $p \geq 1$. This upper limit is always characterized by an unsatisfactory dependence on g, since it is proportional to g^{2p} rather than to g. However, it provides very high accuracy in

[1] From this point and after in this section we will set $U = 2m/\hbar^2 = 1$.

terms of determining the existence of a bound state for a given potential, as we will find in Chapter 3. In 1977, Martin [23] found an upper limit on the number of bound states which features the correct power behavior as $g \to \infty$,

$$N_0 < \left[\int_0^\infty r^2 V^-(r)\, dr \int_0^\infty V^-(r)\, dr \right]^{1/4}. \tag{1.28}$$

After that Chadan et al. [24] have almost filled the gap between the Calogero-Cohn [Eq.(1.24)] and the Bargmann-Schwinger bound [Eq.(1.19)] with:

$$N_l < (2l+1)^{1-2p} p(1-p)^{p-1} \int_0^\infty \frac{dr}{r} |r^2 V(r)|^p, \tag{1.29}$$

with the restriction $1/2 \leq p < 1$, and the potential is nowhere positive and moreover satisfies, for all values of r, the relation:

$$\frac{d}{dr}[r^{1-2p}|V(r)|^{1-p}] \leq 0. \tag{1.30}$$

For $p = 1/2$, it covers Eq.(1.24), and for $p \to 1$ it recovers Eq.(1.19). In 2003, Brau and Calogero [5,6] found new upper and lower limits for the number of bound state energies, which are the so-called Brau and Calogero limits. These limits read

$$N < \frac{\sqrt{U}}{\pi} \int_0^\infty [V^-(r)]^{1/2}\, dr + \frac{1}{4\pi} \ln \left[\frac{V(p)}{V(q)} \right] + \frac{1}{2}, \tag{1.31}$$

$$N > \frac{\sqrt{U}}{\pi} \int_0^\infty [V^-(r)]^{1/2}\, dr - \frac{1}{4\pi} \ln \left[\frac{V(p)}{V(q)} \right] - \frac{3}{2}, \tag{1.32}$$

where p and q are defined as the solutions of the equations

$$\int_0^p [V^-(r)]^{1/2}\, dr = \frac{\pi}{2} \quad \text{and} \quad \int_q^\infty [V^-(r)]^{1/2}\, dr = \frac{\pi}{2}. \tag{1.33}$$

Then, other developments found the upper and lower limits for both the total number of bound state energies and NBSE with better accuracy. For examples, see Refs. [5], [6], [25], [26] [27]. However, these publications are not of interest in this thesis. All limits and equations provided in this section are referred to as the *estimating methods*.

1.4 General treatment for central potentials

The Schrödinger equation in three dimensions for one particle has a potential which may or may not depend on the radius r. If the potential just depends on r, then the potential is called a central potential. The time-independent Schrödinger equation (TISE) in $3D$ has this form:

$$\left[-\frac{1}{U}\bigtriangledown^2 + V(r)\right]\psi = E\psi, \qquad \text{where} \quad U = \frac{2m}{\hbar^2}, \tag{1.34}$$

where $V(r)$ is a central potential. It is clearly convenient to use spherical coordinates, and write the Laplacian as:

$$\bigtriangledown^2 = \frac{1}{r^2}\frac{\partial}{\partial r}\left(r^2\frac{\partial}{\partial r}\right) + \frac{1}{r^2\sin\theta}\frac{\partial}{\partial\theta}\left(\sin\theta\frac{\partial}{\partial\theta}\right) + \frac{1}{r^2\sin^2\theta}\frac{\partial^2}{\partial\phi^2}, \tag{1.35}$$

which can be rewritten as:

$$\bigtriangledown^2 = \frac{1}{r^2}\frac{\partial}{\partial r}\left(r^2\frac{\partial}{\partial r}\right) - \frac{1}{\hbar^2 r^2}\hat{L}^2. \tag{1.36}$$

However, if we do the separation of variables as: $\psi = R(r)Y_l^m(\theta,\phi)$, the function that depends on θ and ϕ is called the spherical harmonic function, and it has this exact expression:

$$Y_l^m(\theta,\phi) = (-1)^m\sqrt{\frac{(2l+1)}{4\pi}\frac{(l-m)!}{(l+m)!}}P_l^m(\cos\theta)e^{im\phi}, \tag{1.37}$$

where l is the azimuthal quantum number which is related to the orbital angular momentum, and m is the magnetic quantum number. It is to be noted that if m is a negative number, the following identity for the associated Legendre polynomial, P_l^m, is satisfied

$$P_l^{-m} = (-1)^m\frac{(l-m)!}{(l+m)!}P_l^m. \tag{1.38}$$

Then, the radial part of Eq.(1.34) becomes:

$$\frac{1}{r^2}\frac{d}{dr}\left(r^2\frac{dR}{dr}\right) - \frac{l(l+1)}{r^2}R + U[E - V(r)]R = 0. \tag{1.39}$$

This equation can be simplified by the substitution:

$$\chi(r) = rR(r). \tag{1.40}$$

Eq.(1.39) then becomes

$$\frac{d^2\chi}{dr^2} + \left[U[E - V(r)] - \frac{l(l+1)}{r^2}\right]\chi(r) = 0, \tag{1.41}$$

and V_{eff} is defined as

$$V_{eff} = V(r) + \frac{l(l+1)}{Ur^2}, \tag{1.42}$$

so that Eq.(1.41) becomes:

$$\frac{1}{U}\frac{d^2\chi}{dr^2} + [E - V_{eff}]\,\chi = 0. \tag{1.43}$$

This equation (1.43) is what we will use to solve the SE for various potentials $V(r)$ for the rest of this thesis.

Now let us turn to the boundary conditions that χ should satisfy. Two boundary conditions are obtained for $R(r)$. First, $R(r)$ has to be finite or have a specific value at the origin. Otherwise, the SE will not be satisfied at the origin, as Shankar [28] has discussed in his book . Second, $R(r)$ has to be zero when $r \to \infty$, that yields

$$\chi(0) = 0, \qquad \text{and} \qquad \chi(\infty) = 0. \tag{1.44}$$

These boundary conditions are very significant since without them we cannot distinguish between physical and non-physical solutions; in addition to these conditions, we will use the continuous conditions in order to determine the physical solution. Also, the normalization condition of χ is written as:

$$\int_0^\infty |\chi(r)|^2\, dr = 1. \tag{1.45}$$

1.5 The plan of this study

In this study we examine the criteria for bound state energies, especially in $3D$ central potentials with l=0. Our main objective is to study NBSE for various attractive potentials and compare the exact properties of NBSE with the estimating methods. Therefore, this study is organized as follows: the first chapter has already introduced the reader to some underlying facts of the criteria for bound state energies, giving a general idea about NBSE in one, two, and three dimensions. The second chapter explains the numerical matrix method, which is the technique we will use to calculate the eigenvalues for potentials that cannot be solved analytically. The third chapter is about comparing

some criteria for bound state energies obtained from the exact soultion of SE, and from the estimating methods for potentials with a finite depth and range. We have used several potentials to show this: the spherical well potential, the triangular potential, Woods-Saxon potential, Yukawa potential, etc. The fourth chapter examines the properties of eigenvalues for potentials that give an infinite number of bound states, and how values of energies differ when we include a cutoff. We have used potentials like the Coulomb potential, square inverse potential, etc. The fifth chapter is devoted to discussion and conclusions.

Chapter 2

Numerical matrix method

In this chapter, we introduce the numerical matrix method which we are going to use in the rest of this thesis for solving the time-independent Schrödinger equation (TISE). Furthermore, this method will be used in this thesis for certain potentials when we cannot solve TISE analytically; moreover, it is applied only to the three dimensional Schrödinger equation with central potentials Sec.(1.4). However, it can be modified to include one or two dimensions [29]. This numerical method provides a practical and direct way to find accurate solutions and thus benefits both students and researchers [30], it can be used on any ordinary personal computer with a software package such as MATLAB, MAPLE, or MATHEMATICA. The idea of the matrix method is based on the notion of embedding the actual potential in an infinite spherical potential well, with a size from $r = 0$ to $r = b$, where b is a sufficiently large cutoff radius.

This chapter will start by explaining the formulation of the matrix mechanics problem. The next section provides two examples of potentials analyzed with the numerical matrix method. Most of this chapter is based on Refs. [29], [30] [31].

2.1 Formulation of the matrix mechanics problem

Let us begin our introduction to the numerical matrix method by recalling the radial Schrödinger equation, Eq.(1.43),

$$\frac{1}{U}\frac{d^2\chi}{dr^2} + [E - V_{eff}]\,\chi = 0, \tag{2.1}$$

where $U = 2m/\hbar^2$, χ is the auxiliary radial function defined as $rR(r)$, and V_{eff} is the effective potential

$$V_{eff} = V(r) + \frac{l(l+1)}{Ur^2}. \tag{2.2}$$

The infinite potential well is defined as

$$V_\infty(r) = \begin{cases} 0 & \text{if } 0 < r < b; \\ \infty & \text{otherwise,} \end{cases} \tag{2.3}$$

where we refer to b as the position of the infinite wall. The well-known eigenstates of this potential are

$$\phi_n(r) = \sqrt{\frac{2}{b}} \sin\left(\frac{n\pi r}{b}\right), \tag{2.4}$$

with eigenvalues

$$E_n^0 = \frac{\pi^2\hbar^2 n^2}{2mb^2} = \frac{\pi^2 n^2}{Ub^2}. \tag{2.5}$$

Then, let us use this eigensystem as a basis with two boundary conditions $\chi(0) = 0$ and $\chi(b) = 0$, so that we can expand our auxiliary radial function χ in terms of ϕ_n. By using the Dirac notation, the radial equation is written as

$$[H_0 + V_{eff}]|\chi\rangle = E|\chi\rangle, \tag{2.6}$$

where H_0 includes both the kinetic energy and the infinite spherical well potential

$$H_0|\phi_n\rangle = E_n^0|\phi_n\rangle. \tag{2.7}$$

Then, let us expand $|\chi\rangle$ in terms of this basis

$$|\chi\rangle = \sum_{m=1}^{\infty} c_m|\phi_m\rangle, \tag{2.8}$$

so that if we substitute this expansion into Eq.(2.6), followed by a product from the left side $\langle\phi_n|$, we will find

$$\sum_{m=1}^{\infty} c_m\langle\phi_n|H_0 + V_{eff}|\phi_m\rangle = \sum_{m=1}^{\infty} c_m\mathbf{H_{nm}} = Ec_n, \tag{2.9}$$

where we have $\langle\phi_n|\phi_n\rangle = 1$, since we already have used normalized eigenstates in Eq.(2.4). The matrix elements are given by

$$\mathbf{H_{nm}} = \langle\phi_n|H_0 + V_{eff}|\phi_m\rangle = \delta_{nm}E_n^0 + \frac{2}{b}\int_0^b \sin\left(\frac{n\pi r}{b}\right) V_{eff} \sin\left(\frac{m\pi r}{b}\right) dr, \tag{2.10}$$

where δ_{nm} is the Kronecker delta function. Also, we rewrite the matrix elements by using this trigonometric identity

$$2\sin a \sin b = \cos(a-b) - \cos(a+b),$$

and Eq.(2.10) becomes

$$\begin{aligned} \mathbf{H_{nm}} &= \delta_{nm}E_n^0 + \tfrac{1}{b}\textstyle\int_0^b V_{eff}\left[\cos\left(\frac{\pi r(n-m)}{b}\right) - \cos\left(\frac{\pi r(n+m)}{b}\right)\right] dr \\ &= \delta_{nm}E_n^0 + \tfrac{1}{b}\textstyle\int_0^b \left(V(r) + \frac{l(l+1)}{Ur^2}\right)\left[\cos\left(\frac{\pi r(n-m)}{b}\right) - \cos\left(\frac{\pi r(n+m)}{b}\right)\right] dr \\ &= \delta_{nm}E_n^0 + \tfrac{1}{b}[F(n-m) - F(n+m)] + \tfrac{1}{b}[K(n-m) - K(n+m)], \end{aligned} \tag{2.11}$$

where $F(m)$ is defined as

$$F(m) = \int_0^b V(r)\left[1 - \cos\left(\frac{\pi r m}{b}\right)\right] dr, \tag{2.12}$$

and $K(m)$ is defined as

$$K(m) = \int_0^b \frac{l(l+1)}{Ur^2}\left[1 - \cos\left(\frac{\pi r m}{b}\right)\right] dr, \tag{2.13}$$

The main advantage of writing the matrix elements $\mathbf{H_{nm}}$ in this formula is to reduce the number of different integrals.

In general, the numerical calculation proceeds as follows: by inserting a potential $V(r)$ into Eq.(2.11), and choosing values of n_{max}, l and b, then evaluating $\mathbf{H_{nm}}$ for all n and m values from 0 to n_{max}. After that, we are able to construct the matrix $\mathbf{H_{nm}}$ and then find its eigenvalues using a standard algorithm. Also, we can find the radial wave function as

$$R_{n,l}(r) = \frac{1}{r}\sum_{m=1}^{n_{max}} c_m^{(n,l)}\sqrt{\frac{2}{b}}\sin\left(\frac{m\pi r}{b}\right). \tag{2.14}$$

Two issues should be clarified before we provide some examples. First, the size of the matrix in Eq.(2.9) is infinite. We will make the matrix finite by imposing an upper cutoff n_{max}, which will be inserted in Eq.(2.14). However, we are going to increase n_{max} until the results have converged. Therefore, we omit the high-energy states of high n, since they have weak contributions compared

to the actual low-energy bound states, which we are looking for. Second, the width of the infinite wall b should be many times larger than the natural length scale of the system. However, increasing b requires that we increase n_{max} in order to keep the accuracy high enough. We will observe such a behaviour in the next couple of examples.

2.2 Examples

Two potentials were used to illustrate the numerical method in practice. The first potential is the finite spherical well which has a finite depth for all its domain. The second potential is the Coulomb potential which has an infinite depth at the origin and infinite range.

2.2.1 The finite spherical well

The finite spherical well is defined as the following

$$V_{sph}(r) = \begin{cases} -V_0 & \text{if } 0 < r < R; \\ 0 & \text{otherwise.} \end{cases} \tag{2.15}$$

By applying the definition of this potential and substituting $l = 0$ into Eq.(2.11), we find the matrix elements $\mathbf{H_{nm}}$ as:

$$\mathbf{H_{nm}} = \delta_{nm} E_n^0 - \frac{V_0}{\pi}[g(n-m) - g(n+m)], \tag{2.16}$$

where, as before, $E_n^0 = (\pi^2 n^2)/(Ub^2)$ and

$$g(n) = \frac{\sin(n\pi R/b)}{n}, \tag{2.17}$$

with $g(0) = \pi R/b$ as implied by L'Hôpital's rule.

The spherical potential well has a fixed number expression $\mathbf{G}$ defined on page 4. However, we will show in Ch.(3), Sec.(3.2.1), that the fixed number expression $\mathbf{G_{sph}}$ of the spherical potential well is

$$\mathbf{G}_{sph} = UR^2V_0. \tag{2.18}$$

In any event, if the expression (2.18) is fixed and we vary R, V_0 and U, we will always get the same number of bound state energies. Our purpose, when using this matrix method for this potential, is

to find the critical value of $\mathbf{G^c_{sph}}$ which is defined in Sec.(1.3). Consequently, in order to do that we have to find some values of $\mathbf{G^c_{sph}}$ for certain values of the size of the infinite wall b. Then, we find the asymptotic behaviour as $b \to \infty$.

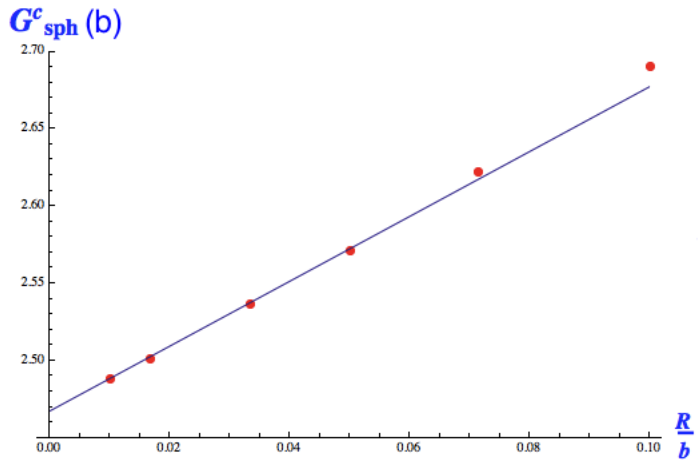

Figure 2.1: (Color line) A plot of $\mathbf{G^c_{sph}}$, the critical value of $\mathbf{G_{sph}}$ below which a bound state energy no longer exists, vs. R/b. As $b \to \infty$ the effect of the infinite wall becomes negligible. The plot shows a linear relationship with a cross point in the y-axis equal to 2.4674, which agrees with the well-known analytical result $\pi^2/4$, see Sec.(3.2.1).

From Figure 2.1, it is clear that when $b \to \infty$, (R/b) intersects with the y-axis at approximately 2.467 which is in good agreement with the well-known exact value $\pi^2/4$. Therefore, this indicates a success of this numerical matrix method. For a potential with a finite number of bound states, the programme almost follows a similar approach to this example for which the intersection with the y-axis gives the exact value.

2.2.2 The Coulomb potential

Another example is the Coulomb potential which has the definition

$$V_{coul}(r) = -\frac{e^2}{4\pi\epsilon_0}\frac{1}{r} = -\frac{A}{r}, \tag{2.19}$$

where A is $e^2/4\pi\epsilon_0$, or could be any other positive value. The Coulomb potential has an infinite range and infinite depth at the origin. We want to know how the numerical matrix method deals with such a potential. Let us begin by applying this potential to Eq.(2.11) for the $l = 0$ case to

obtain the following matrix elements

$$\mathbf{H_{nm}} = \delta_{nm} E_n^0 - \frac{A}{b}[F_{coul}(n+m) - F_{coul}(n-m)], \tag{2.20}$$

where

$$F_{coul}(m) = \int_0^1 \frac{1-\cos(m\pi x)}{x}\, dx. \tag{2.21}$$

We already know the ground state energy of the Coulomb potential,

$$E_{coul}^0 = -\frac{e^4 U}{64\pi^2 \epsilon_0^2} = -\frac{A^2 U}{4}. \tag{2.22}$$

Also, we know the Bohr radius

$$a_0 = \frac{8\pi\epsilon_0}{Ue^2} = \frac{2}{UA}. \tag{2.23}$$

Then, if we normalize Eq.(2.20) to the Coulomb ground state energy, and substitute the Bohr radius, we will find

$$h_{nm} = \frac{\mathbf{H_{nm}}}{|E_{coul}^0|} = \delta_{nm}\left(\frac{\pi n a_0}{b}\right)^2 - \frac{2a_0}{b}[F_{coul}(n+m) - F_{coul}(n-m)]. \tag{2.24}$$

n_{max}	b/a_0	ϵ_1	ϵ_2	ϵ_3	ϵ_4	ϵ_5
50	5	−0.992728	+	+	+	+
50	10	−0.999208	−0.225474	+	+	+
50	20	−0.994276	−0.249248	−0.0995125	+	+
50	50	−0.941139	−0.242071	−0.108718	−0.0613726	−0.0348543
100	10	−0.999894	−0.225594	+	+	+
100	20	−0.999198	−0.249874	−0.0997914	+	+
100	50	−0.989317	−0.248637	−0.110705	−0.0622342	−0.0355843
100	100	−0.940482	−0.241978	−0.10869	−0.0614704	−0.0394705
500	20	−0.999993	−0.249973	−0.0998357	+	+
500	50	−0.999894	−0.249987	−0.111107	−0.062407	−0.0357281
500	90	−0.999403	−0.249925	−0.111089	−0.0624906	−0.0399943
500	150	−0.997388	−0.249671	−0.111013	−0.0624588	−0.0399789

Table 2.1: Results of the Coulomb potential with $l = 0$, where ϵ_n is the energy obtained from the programme divided by E_{coul}^0, and + means positive results. The exact results of ϵ_n are $\epsilon_1 = -1$, $\epsilon_2 = -0.25$, $\epsilon_3 = -1/9$, $\epsilon_4 = -0.0625$ and $\epsilon_5 = -0.04$. A very high accuracy is obtained for the energy spectrum when both n_{max} and b have high values.

From Table 2.1, we find that when we increase b/a_0, the number of bound state energies increases as well, and when we increase n_{max}, we increase the accuracy. However, if we want to get a very high accuracy for the first few energies, we can use small values of b/a_0 with high n_{max}; also, if we wish to cover more energies of the infinite spectrum of the Coulomb eigenvalues, we can use high values of b/a_0 and high n_{max}. Therefore, the results obtained with this method depend on priorities: for rapid computations, one should use small n_{max}, for high accuracy, one should take b/a_0 small, and in order to obtain more energies with a high accuracy, one should use high value of b/a_0, and correspondingly high values of n_{max}. However, for potentials that have an infinite number of bound states, the programme follows a similar approach to the Coulomb potential.

Chapter 3

Potentials with a finite number of bound states

In this chapter, we solve the time-independent Schrödinger equation (TISE) in $3D$ for $l = 0$ with various potentials, where all these potentials are central and have a finite number of bound state energies (NBSE). Solving TISE for these potentials aims to determine the main characteristics of the bound state energies such as: the fixed number expression (FNE), the critical conditions, the lower and upper limits on NBSE, etc. Once we know the exact behavior for a given criterion, we will test some of the estimating methods to see which one is closer to the exact behavior. To do that, we have to define and discuss each one of these criteria as we will do in Section 3.1.

We have organized this chapter by setting the first section to describe the general concepts of the finite NBSE and some of its estimating methods. The second section considers potentials with two parameters and provides some physical examples: the finite spherical potential, the triangular potential, and the Yukawa potential. The third section deals with potentials with three parameters with the following examples: the finite spherical potential shell, the cutoff triangular potential, and the Woods-Saxon potential.

3.1 General outlines

In this section, we will provide the main criteria for our examination of the bound state energies which they we will utilize in this chapter. Also, some of the estimating methods will be compared.

First, let us present the fixed number expression (FNE) $\mathbf{G}$, starting by recalling its definition from Ch.(1) in section 1.1, which is:

For a given potential there exists an expression which will be a function of the potential's parameters; if this expression is fixed, the number of bound state energies will be fixed as well, so if we know it, we can write $N = f(\mathbf{G})$.

One of the main statements of this thesis is that the FNE is important and simplifies the presentation of results of NBSE. Therefore, we have provided this expression for all potentials solved in this chapter. The main method to determine the FNE for a potential is to solve SE and find the final energy equation, and from this equation we can define the FNE. Also, for potentials having two parameters, we can use the estimating methods which directly provides FNE; on the other hand, these methods do not provide an exact FNE for potentials with three parameters. We do not have any evidence that for any potential FNE this will be same for all values of (l) and in all spatial dimensions. However, if we know FNE for a given potential, we can fix it and vary its parameters without changing NBSE. Now, let us turn to the main property of $(\mathbf{G})$ which is writing FNE in the form of basic mathematical function such as, square root, nth power, etc, and will not effect the fact that NBSE remains unchanged, just if $f(\mathbf{G})$ is fixed. In other words,

$$\mathbf{G} \equiv f(\mathbf{G}), \tag{3.1}$$

where f is any basic monotonic increasing function. The only difference that exists between one FNE and another is the range of the results, as we will find in the third section. Therefore, we try to represent the FNE by means of the simplest formula. The estimating methods we will test are the Calogero and Cohn upper limit, Eq.(1.24), and the Bargmann-Schwinger bound, Eq.(1.19).

Second, let us recall the critical point $\mathbf{G^c}$ which is defined in Ch.(1) in Sec.(1.3) as:

For the $3D$ *SE, for a given attractive potential with a finite number of bound state energies (NBSE), there exists a constant number* $\mathbf{G^c}$ *which, if we make* $\mathbf{G}$ *in Def.(1) higher than this number, will result in at least one bound state, and for* $\mathbf{G}$ *lower than this number there will be no bound state.*

The critical point is important when studying the $3D$ SE since it is one of the main differences between the $1D$ and the $3D$ SE. However, when $\mathbf{G}$ has a complicated form, as in potentials having three parameters, it is easier to study the critical curve rather than the critical point.

Definition 3. The critical curve ($\mathbf{W_c}$)

For some potentials in the 3D SE, it is possible to define the critical curve, which describes the dependence of some of the potential parameters ($\mathbf{W_c}$) as a function of other parameters of the potential ($\mathbf{g}$), so each point of this curve can be understood as one trivial critical point $\mathbf{G^c_{trivial}}$ for those parameters.

Then, we will obtain the critical conditions from the analytical solution for SE, or from the numerical solutions if we are unable to solve SE. In addition, the estimating method we are going to use to determine the critical conditions is the generalized Bargmann-Schwinger bound.

Since we are going to use the generalized B-S bound in this chapter frequently, we will provide a quick proof for this method. For more details see [7]. As we already know the radial SE can be written as

$$\left(-\frac{1}{U}\frac{d^2}{dr^2}+\frac{l(l+1)}{r^2}\right)\chi(r)=[E-V(r)]\chi(r), \tag{3.2}$$

where $\chi(r)$ are the eigenstates and E are the eigenvalues. Let $G(r,r')$ be the Green's function for the kinetic operator:

$$\left(-\frac{1}{U}\frac{d^2}{dr^2}+\frac{l(l+1)}{r^2}\right)G(r,r')=\delta(r-r'), \tag{3.3}$$

where $\delta(x)$ is the usual delta function. The Green's function, $G(r,r')$ of the kinetic energy operator takes the explicit form

$$G(r,r')=\frac{U}{2l+1}r_<^{l+1}r_>^{-l}, \tag{3.4}$$

where $r_<=\min[r,r']$ and $r_>=\max[r,r']$. In the case $E=0$, we can write

$$\chi(r)=-\int G(r-r')V(r)\chi(r')\,dr'. \tag{3.5}$$

The purpose of this method is to find an upper limit for the NBSE. We can replace $V(r)$ by $-V^-(r)$ where $V^-(r)$ is the absolute value of the negative part of the potential. Let us introduce the parameter $0<\lambda\leq 1$ by the substitution $V^-(r)\rightarrow\lambda V^-(r)$. As λ increases from 0, we reach a critical value, λ_1, for which the first bound state appears with $E=0$. By further growth of λ, we will reach the second critical value λ_2, for which the second bound state appears with $E=0$, and so on. When λ reaches the value unity and $\lambda_N\geq 1<\lambda_{N+1}$, there are N bound states.

Let us introduce $\Phi(r)$:

$$\Phi(r)=[V^-(r)]^{1/2}\chi(r). \tag{3.6}$$

Then, Eq.(3.5) becomes

$$\Phi(r) = \lambda \int K(r, r')\Phi(r')dr', \tag{3.7}$$

where $K(r, r')$ is the symmetric kernel,

$$K(r, r') = [V^-(r)]^{1/2} G(r, r')[V^-(r')]^{1/2}; \qquad K(r, r') = K(r', r). \tag{3.8}$$

If the kernel is positive, we have $0 < \lambda_1 < \lambda_2 < \ldots \lambda_N \leq 1$ and $0 < \lambda_k < \infty$, where λ_k denotes each eigenvalue of Eq.(3.7). From Mercer's theorem in the functional analysis, it is known that the trace of the iterated kernels equals the sum of the eigenvalues of the integral equation Eq.(3.7) see [43]

$$\sum_{k=1}^{\infty} \frac{1}{(\lambda_k)^n} = \int K^{(n)}(r, r)dr, \tag{3.9}$$

where the iterated kernel $K^{(n)}(s, t)$ is given by

$$K^{(n)}(s, t) = \int K(s, u)K^{(n-1)}(u, t)du, \tag{3.10}$$

with

$$K^{(1)}(s, t) \equiv K(s, t). \tag{3.11}$$

It is obvious from $0 < \lambda_1 < \lambda_2 < \ldots \lambda_N \leq 1$, and $0 < \lambda_k < \infty$ that the following inequalities hold

$$\sum_{k=1}^{\infty} \frac{1}{(\lambda_k)^n} \geq \sum_{k=1}^{N} \frac{1}{(\lambda_k)^n} > N, \tag{3.12}$$

where N is NBSE, from the previous equations we can write

$$N < \int K^{(n)}(r, r)\, dr. \tag{3.13}$$

Schwinger considered only the case $n = 1$ for Eq.(3.13) which yields Eq.(1.19). However, increasing n gives worse results to this upper limit, but we want here to determine the critical conditions, which means replacing $N = 1$, and then Eq.(3.13) will usually be called the necessary conditions for the existence of l-wave bound state. Also, we want it for $l = 0$. Here we provide $n = 1, 2, 3$ respectively

for Eq.(3.13)

$$1 \leq U \int_0^\infty r V^-(r)\, dr, \tag{3.14}$$

$$1 \leq 2U^2 \int_0^\infty V^-(r_1)\, dr_1 \int_0^{r_1} V^-(r_2) r_2^2\, dr_2, \tag{3.15}$$

$$1 \leq 6U^3 \int_0^\infty V^-(r_1)\, dr_1 \int_0^{r_1} V^-(r_2) r_2\, dr_2 \int_0^{r_2} V^-(r_3) r_3^2\, dr_3. \tag{3.16}$$

We can provide more terms in order to get a higher accuracy, but for the purpose of this thesis, these three equations are sufficient.

The third criterion is the lower and upper limits which are one of our topics in this chapter. We can use one of the limits provided in Ch.(1) to represent the lower and upper limits. However, we want to use one of the most accurate and recent one to find these limits. Brau and Calogero [32] found the upper and lower limits for the $3D$ SE for attractive monotonically increasing potentials Eqs.(1.31, 1.32). The limits read

$$N < \frac{\sqrt{U}}{\pi} \int_0^\infty [V^-(r)]^{1/2}\, dr + \frac{1}{4\pi} \ln\left[\frac{V(p)}{V(q)}\right] + \frac{1}{2}, \tag{3.17}$$

$$N > \frac{\sqrt{U}}{\pi} \int_0^\infty [V^-(r)]^{1/2}\, dr - \frac{1}{4\pi} \ln\left[\frac{V(p)}{V(q)}\right] - \frac{3}{2}, \tag{3.18}$$

where p and q are defined as the solutions of the equations

$$\int_0^p [V^-(r)]^{1/2}\, dr = \frac{\pi}{2} \quad \text{and} \quad \int_q^\infty [V^-(r)]^{1/2}\, dr = \frac{\pi}{2}. \tag{3.19}$$

We are going to use these limits in the rest of this chapter except for the finite spherical shell potential, since it is not a monotonic potential. Also, for potentials that cause some difficulty to determine p or q, we will neglect the second terms of equations (3.17) and (3.18) as for the Woods-Saxon potential.

The final issue we wish to discuss is the continuity conditions and the energy equation. The well-known requirement is that the radial wave function $R(r) = \psi(r)$ and its derivative $R'(r) = \psi'(r)$ need to be continuous functions over their entire range. Therefore, if we know the radial wave function $\psi_1(r)$ in the range $(0, R_0)$ and $\psi_2(r)$ in the range (R_0, ∞), then we can write the continuity

conditions as follows:

$$\psi_1(R_0) = \psi_2(R_0) \qquad\qquad \psi_1'(R_0) = \psi_2'(R_0). \tag{3.20}$$

These two continuity conditions can be written into one formula as

$$\frac{\psi_1'(R_0)}{\psi_1(R_0)} = \frac{\psi_2'(R_0)}{\psi_2(R_0)}. \tag{3.21}$$

Also, to solve SE we have to consider the boundary conditions discussed in Ch.(1). Then, the final step in solving SE for a potential is to find the final energy equation which includes all the criteria of bound state energies. In the next section, we consider potentials with two parameters.

3.2 Two-parameter potentials

Potentials with two parameters have some interesting properties. One of these properties is the FNE. We know that any potential for SE has FNE which, if it is fixed, will correspond to a fixed NBSE as well. However, with two parameters, there exists an additional property which is that for a certain normalization of the eigenvalues ($\epsilon_n = E_n/E_{norm}$), where E_{norm} is a certain normalization, the normalized energy (ϵ_n) will always be the same if FNE is fixed. To illustrate this point, we provide a simple illustration. Let $V_2(r)$ be a potential with two parameters which can be written as $V_0 f(r/R_0)$, where V_0 and R_0 are the two parameters which correspond to the depth and the range of the potential, respectively, and f is some mathematical function. The radial SE can be written as

$$-\frac{1}{U}\frac{d^2\psi}{dr^2} + V_0 f(r/R_0)\psi = E\psi. \tag{3.22}$$

By changing the variables to $r = zR_0$, it gives

$$-\frac{1}{UV_0R_0^2}\frac{d^2\psi}{dz^2} + f(z)\psi = \left(\frac{E}{V_0}\right)\psi. \tag{3.23}$$

This equation indicates the following

$$\frac{E}{V_0} = f_1(UV_0R_0^2), \tag{3.24}$$

where f_1 is some function. Eq.(3.24) tells us that if we fixed the expression ($\mathbf{G} = UV_0R_0^2$) which is the FNE, we will always get the same value of the normalized energy which is (E/V_0).

In this section, we will provide the critical point, the upper and lower limits for each potential that is studied. We have solved two potentials analytically, they are the regular finite spherical potential and the triangular potential. Also, we have solved one potential numerically which is the Yukawa potential.

3.2.1 Finite spherical potential well

The finite spherical potential is very important in physics and has many applications such as: quantum dots, simplified nuclear models, etc. Also, we are going to use this potential more than once in this thesis because when imposing a cutoff in a potential, we actually realize the finite spherical potential. It is defined as

$$V_{sph}(r) = \begin{cases} -V_0 & \text{if } 0 < r < R_0; \\ 0 & \text{otherwise,} \end{cases} \tag{3.25}$$

and looks like

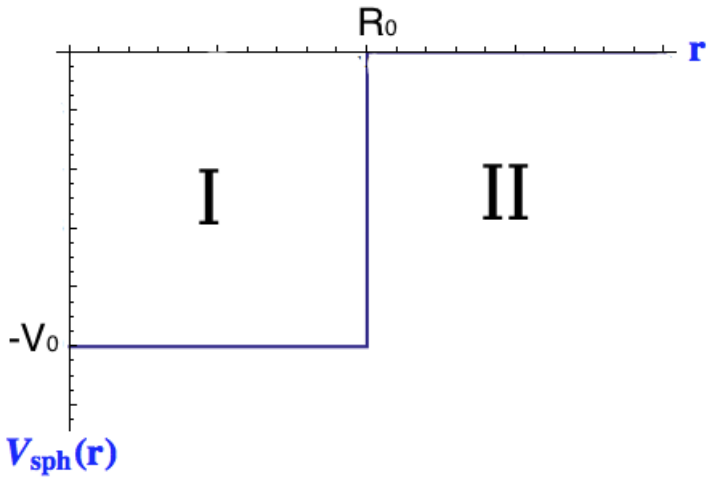

Figure 3.1: The regular spherical potential, where **I** is the first region and **II** is the second region. V_0 is the depth, and R_0 is the range of this potential.

Now, we want to solve SE for the case $l = 0$. Therefore, let us recall the radial SE Eq.(1.43) for

the first region **I**.

$$\frac{1}{U}\frac{d^2\chi_1}{dr^2} + [E + V_0]\,\chi_1 = 0, \tag{3.26}$$

where U is $2m/\hbar^2$, and χ_1 is the auxiliary radial wave function $r\psi_1(r)$. The general solution of this differential equation (DE) is

$$\chi_1(r) = a_1 \sin(qr) + a_2 \cos(qr), \qquad q = \sqrt{U(E + V_0)}. \tag{3.27}$$

The second term must be removed because it does not satisfy the boundary condition $\chi(0) = 0$. Then, the radial wave function is

$$\psi_1(r) = \frac{a_1 \sin(qr)}{r}. \tag{3.28}$$

The derivative of $\psi_1(r)$ is

$$\psi_1'(r) = a_1 \left(\frac{qr\cos(qr) - \sin(qr)}{r^2} \right). \tag{3.29}$$

By combining Eq.(3.28) and Eq.(3.29), we get

$$\frac{\psi_1'(r)}{\psi_1(r)} = q\cot(qr) - \frac{1}{r}. \tag{3.30}$$

Then, SE of the second region **II** is

$$\frac{1}{U}\frac{d^2\chi_2}{dr^2} + E\chi_2 = 0, \tag{3.31}$$

the solution of this DE is given by

$$\chi_2 = b_1 e^{-kr} + b_2 e^{kr}, \qquad k = \sqrt{-UE}. \tag{3.32}$$

The second term does not satisfy the second boundary condition $\chi(\infty) = 0$, so we will omit it. The radial function is given by

$$\psi_2 = \frac{b_1 e^{-kr}}{r}. \tag{3.33}$$

Then, its derivative is:

$$\psi_2' = -\frac{b_1(kr + 1)\exp(-kr)}{r^2}, \tag{3.34}$$

and by dividing Eq.(3.34) by Eq.(3.33), we will get

$$\frac{\psi_2'(r)}{\psi_2(r)} = -k - \frac{1}{r}. \tag{3.35}$$

Now, let us apply the continuity conditions by equating Eq.(3.30) to Eq.(3.35) at R_0. We find:

$$q\cot(qR_0) - \frac{1}{R_0} = -k - \frac{1}{R_0}. \tag{3.36}$$

By defining $\epsilon = E/V_0$ and rearranging Eq.(3.36), we find

$$\cot\left[\sqrt{UR_0^2V_0(\epsilon+1)}\right] = -\sqrt{\frac{-\epsilon}{\epsilon+1}}. \tag{3.37}$$

This is the energy equation of the finite spherical potential. We can find the value of the energies (ϵ_n) by plotting both the right-hand side (RHS), and the left-hand side (LHS) in the same plot with respect to ϵ. Then, by finding the intersection points, these intersection points represent the exact value of ϵ_n. The range of ϵ is between -1 to 0.

From Eq.(3.37) we can define the FNE as

$$\mathbf{G_{sph}} = UR_0^2V_0. \tag{3.38}$$

Obviously, if we fix it and vary R_0, V_0 or U, so that $\mathbf{G_{sph}}$ is fixed, we always will get the same NBSE, and we will get exactly the same values of ϵ_n. Accordingly, what makes NBSE of one spherical potential differ from another spherical potential is the value of $\mathbf{G_{sph}}$.

Now, let us turn to the determination of the exact expression of NBSE for this potential. We can do that by setting ϵ to zero in Eq.(3.37). Then, we will find

$$\begin{aligned}
\cot\left(\sqrt{UR_0^2V_0}\right) &= 0, \\
\sqrt{UR_0^2V_0} &= (N-\tfrac{1}{2})\pi, \\
N &= \left[\tfrac{1}{\pi}\sqrt{UR_0^2V_0} + \tfrac{1}{2}\right], \\
N &= \left[\tfrac{\sqrt{\mathbf{G_{sph}}}}{\pi} + \tfrac{1}{2}\right],
\end{aligned} \tag{3.39}$$

where $[Q]$ means the nearest integer less than the value of Q. The above equation indicates NBSE N for the finite spherical potential. Let us compare Eq.(3.39) with the one of the estimating methods

which is the upper and lower limits of Eq.(3.17, 3.18). We found

$$\begin{aligned} N &< \frac{\sqrt{UR_0^2V_0}}{\pi} + \frac{1}{2} \\ N &> \frac{\sqrt{UR_0^2V_0}}{\pi} - \frac{3}{2}, \end{aligned} \tag{3.40}$$

where we have neglected the term that includes p and q. The upper limit is exactly the same as the analytical expression which means this upper limit is very precise for this potential. In addition to that, we can find the exact critical point of this potential by setting $N = 1$ in Eq.(3.39), and solve it for ($\mathbf{G_{sph}}$). We obtain:

$$\mathbf{G^c_{sph}} = UR_0^2V_0 = \frac{\pi^2}{4} = 2.4674011\cdots . \tag{3.41}$$

This value means that if $\mathbf{G_{sph}}$ is lower than $\pi^2/4$, there will not be any bound state. Let us compare this analytical critical point with the estimating one by using equations (3.14, 3.15, 3.16), respectively:

$$\begin{aligned} 1 &\leq \frac{UR_0^2V_0}{2}, && \Rightarrow \mathbf{G^c_{sph}} = 1.41421, \\ 1 &\leq \frac{U^2V_0^2R_0^4}{6}, && \Rightarrow \mathbf{G^c_{sph}} = 2.44949, \\ 1 &\leq \frac{U^3V_0^3R_0^6}{15}, && \Rightarrow \mathbf{G^c_{sph}} = 2.46621. \end{aligned} \tag{3.42}$$

These equations give very high accuracy in determining the critical point ($\mathbf{G^c_{sph}}$) for the finite spherical potential. For example, the third equation of the necessary conditions gave accuracy up to 99.95% to the exact value.

The last thing we wish to show for this potential is an approximate expression for the value of energies. This approximation is for large values of $\mathbf{G_{sph}} >> 1$, then Eq.(3.37) becomes:

$$\begin{aligned} \cot[\sqrt{\mathbf{G_{sph}}(1+\epsilon)}] &\approx \infty, \\ \sqrt{\mathbf{G_{sph}}(\epsilon+1)} &\approx n\pi, \\ \epsilon_n &= \frac{n^2\pi^2}{\mathbf{G_{sph}}} - 1, \\ E_n &= \frac{n^2\pi^2}{UR_0^2} - V_0. \end{aligned} \tag{3.43}$$

These energies are similar to the infinite spherical well eigenvalues.

3.2.2 Triangular potential

This potential has some applications in physics such as the cold emission of electrons from a metal in the absence of any external electric field [2]. Since this potential is finite, it has a finite NBSE.

The potential is defined as

$$V_{tri}(r) = \begin{cases} V_0 \left(\frac{r}{R_0} - 1\right) & \text{if } 0 < r < R_0; \\ 0 & \text{if } r > R_0, \end{cases} \tag{3.44}$$

and looks like a triangle.

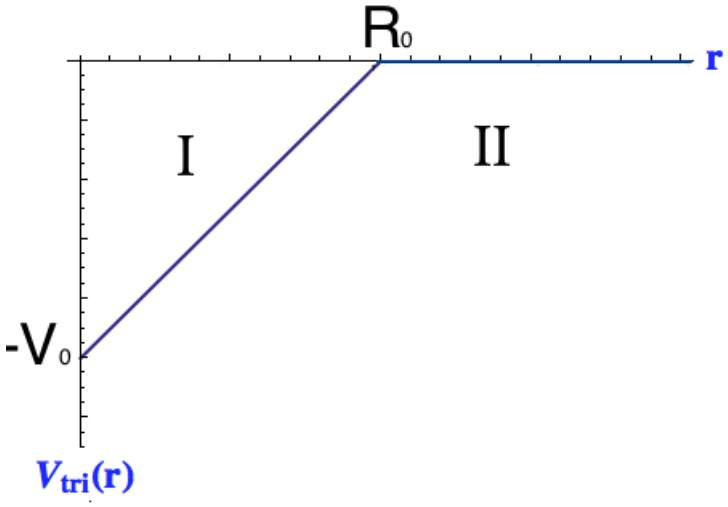

Figure 3.2: The triangular potential, where **I** is the first region, and **II** is the second region. R_0 its range, and V_0 is its depth.

First, let us solve the SE for the first part of this potential **I**. SE reads

$$\frac{1}{U}\frac{d^2\chi_1}{dr^2} + \left[E - V_0\left(\frac{r}{R_0} - 1\right)\right]\chi_1 = 0, \tag{3.45}$$

which can be rewritten as

$$-\frac{1}{U}\frac{d^2\chi_1}{dr^2} + \frac{V_0}{R_0}r\chi_1 = (V_0 + E)\chi_1. \tag{3.46}$$

Now, let us change the variables to

$$r = \rho y + \sigma, \tag{3.47}$$

with

$$\rho = \left(\frac{R_0}{UV_0}\right)^{\frac{1}{3}}, \qquad \sigma = \frac{(V_0 + E)R_0}{V_0} = (1 + \epsilon)R_0, \tag{3.48}$$

where ϵ is E/V_0. Then, Eq.(3.46) becomes

$$\frac{d^2\chi_1}{dy^2} = y\chi_1. \tag{3.49}$$

This equation is known as the Airy differential equation [33], and its general solution is

$$\chi_1(r) = a_1 Ai(y) + a_2 Bi(y), \tag{3.50}$$

where Ai and Bi are the Airy functions, with definitions as integral representations,

$$\begin{array}{rcl} Ai(x) & = & \frac{1}{\pi}\int_0^\infty \cos\left(\frac{t^3}{3} + xt\right)\, dt \\ Bi(x) & = & \frac{1}{\pi}\int_0^\infty \left[\exp\left(-\frac{t^3}{3} + xt\right) + \sin\left(\frac{t^3}{3} + xt\right)\right]\, dt. \end{array} \tag{3.51}$$

Then, the radial wave function is

$$\psi_1(r) = \frac{a_1 Ai\left(\frac{r-\sigma}{\rho}\right) + a_2 Bi\left(\frac{r-\sigma}{\rho}\right)}{r}, \tag{3.52}$$

and its derivative is

$$\psi_1'(r) = \frac{a_1 r Ai'\left(\frac{r-\sigma}{\rho}\right) - a_1\rho Ai\left(\frac{r-\sigma}{\rho}\right) + a_2 r Bi'\left(\frac{r-\sigma}{\rho}\right) - a_2\rho Bi\left(\frac{r-\sigma}{\rho}\right)}{\rho r^2}, \tag{3.53}$$

where Ai' and Bi' are the first derivative of the Airy functions with respect to their argument. By dividing Eq.(3.53) by Eq.(3.52), we obtain

$$\frac{\psi_1'(r)}{\psi_1(r)} = \frac{CAi'\left(\frac{r-\sigma}{\rho}\right) + Bi'\left(\frac{r-\sigma}{\rho}\right)}{\rho\left[CAi\left(\frac{r-\sigma}{\rho}\right) + Bi\left(\frac{r-\sigma}{\rho}\right)\right]} - \frac{1}{r}, \tag{3.54}$$

where C is a_1/a_2. Let us turn to the second region **II** of this potential. We already have solved this region and obtained its condition

$$\frac{\psi_2'(r)}{\psi_2(r)} = -k - \frac{1}{r}, \qquad k = \sqrt{-UE}. \tag{3.55}$$

Let us now apply the continuity condition at R_0 which consists in equating Eq.(3.54) to Eq.(3.55).

We find

$$\frac{CAi'\left(\frac{R_0-\sigma}{\rho}\right)+Bi'\left(\frac{R_0-\sigma}{\rho}\right)}{\rho\left[CAi\left(\frac{R_0-\sigma}{\rho}\right)+Bi\left(\frac{R_0-\sigma}{\rho}\right)\right]}=-k. \tag{3.56}$$

Then, in order to determine the coefficient C, we have another condition which is $\chi_1(0)=0$, so

$$CAi\left(\frac{-\sigma}{\rho}\right)+Bi\left(\frac{-\sigma}{\rho}\right)=0. \tag{3.57}$$

By defining $\frac{R_0-\sigma}{\rho}\equiv-\theta\epsilon$, $\frac{-\sigma}{\rho}\equiv-(1+\epsilon)\theta$, and $k\rho\equiv\sqrt{-\epsilon\theta}$, and combining both continuity conditions Eqs.(3.56) and (3.57), we finally get

$$\frac{Ai(-(1+\epsilon)\theta)\left[Bi'(-\theta\epsilon)+\sqrt{-\theta\epsilon}Bi(-\theta\epsilon)\right]}{Bi(-(1+\epsilon)\theta)\left[Ai'(-\theta\epsilon)+\sqrt{-\theta\epsilon}Ai(-\theta\epsilon)\right]}=1, \tag{3.58}$$

where

$$\theta=(UV_0R_0^2)^{1/3}. \tag{3.59}$$

This equation is the energy equation for this potential. From this equation we are able to find all the criteria for bound state energies. We concentrate on the cases when $\epsilon\to0$; in which case Eq.(3.58) becomes

$$\frac{Ai(-\theta)\,Bi'(0)}{Bi(-\theta)\,Ai'(0)}=\frac{-\sqrt{3}Ai(-\theta)}{Bi(-\theta)}=1, \tag{3.60}$$

where $Bi'(0)/Ai'(0)$ is equal to $-\sqrt{3}$. Let us replace θ in the previous equation by its value, and so we find

$$\sqrt{3}Ai\left[-(UV_0R_0^2)^{1/3}\right]+Bi\left[-(UV_0R_0^2)^{1/3}\right]=0. \tag{3.61}$$

Second, we determine the FNE of this potential from Eq.(3.61) or Eq.(3.58). This potential, as any two parameters potentials, has an obvious FNE which is

$$\mathbf{G_{tri}}=UV_0R_0^2. \tag{3.62}$$

This FNE is exactly the same FNE as the regular finite spherical potential. Furthermore, we are able to determine the critical point from Eq.(3.61), and the first solution of this equation leads to

$$\mathbf{G_{tri}^c}=7.8373\cdots. \tag{3.63}$$

Then, let us try to compare this exact result with the estimating methods of the necessary conditions Eqs.(3.14), (3.15) and (3.16); we will find

$$\begin{aligned} 1 &\leq \frac{UR_0^2V_0}{6}, && \Rightarrow \mathbf{G^c_{tri}} = 6, && Eq.(3.14); \\ 1 &\leq \frac{U^2V_0^2R_0^4}{60}, && \Rightarrow \mathbf{G^c_{tri}} = 7.74597, && Eq.(3.15); \\ 1 &\leq \frac{U^3V_0^3R_0^6}{480}, && \Rightarrow \mathbf{G^c_{tri}} = 7.82974, && Eq.(3.16), \end{aligned} \tag{3.64}$$

the third one clearly gives a very high accuracy to the exact critical condition. For example, the last one gives an accuracy up to 99.9% which is considered to be sufficiently high precision. Next, let us apply Eqs.(3.17, 3.18) to find the upper and lower limits to this potential:

$$\begin{aligned} N &< \frac{2\sqrt{UV_0R_0^2}}{3\pi} + \frac{1}{2} = \frac{2\sqrt{\mathbf{G_{tri}}}}{3\pi} + \frac{1}{2}; \\ N &> \frac{2\sqrt{UV_0R_0^2}}{3\pi} - \frac{3}{2} = \frac{2\sqrt{\mathbf{G_{tri}}}}{3\pi} - \frac{3}{2}, \end{aligned} \tag{3.65}$$

where we have neglected p and q. From Figure 3.3 we can see how close the upper limit is to the exact values of critical points of NBSE.

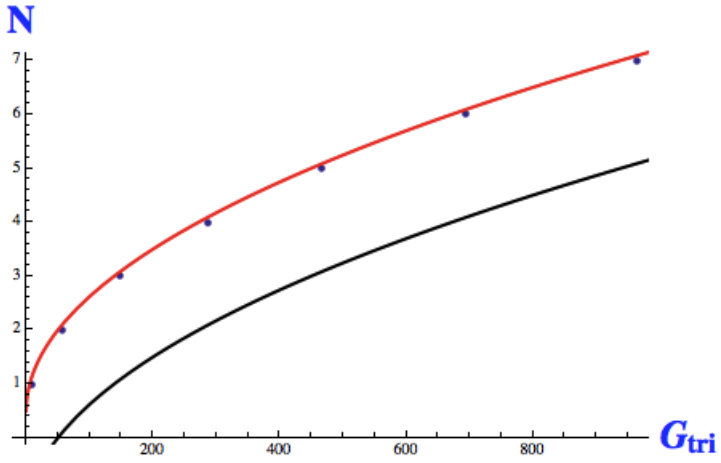

Figure 3.3: NBSE in the triangular potential, where the red curve indicate the upper limit of Eq.(3.65), and the black line is the lower limit of Eq.(3.65). The blue points are the exact value of critical NBSE, obtained from Eq.(3.61). These points means that if $(\mathbf{G^i_{tri}}, N^i)$ is a critical point in NBSE, then if $(\mathbf{G_{tri}})$ is less than $(\mathbf{G^i_{tri}})$ the NBSE (N^i) will not exist, and if it is more than $(\mathbf{G^i_{tri}})$ the NBSE (N^i) will exist.

3.2.3 Yukawa potential

The Yukawa potential has many applications in condensed matter and nuclear physics. It is also called the screened Coulomb potential, and the regular Coulomb potential is a particular case of a Yukawa potential with $e^{-\mu r} = 1$. This potential has not been solved analytically without using an approximation [35]; therefore, we are going to compute the numerical matrix method to get the value of its energy. The definition of this potential is

$$V_{yu} = -\frac{A}{r} e^{-\mu r}, \tag{3.66}$$

which is shown in Figure 3.4.

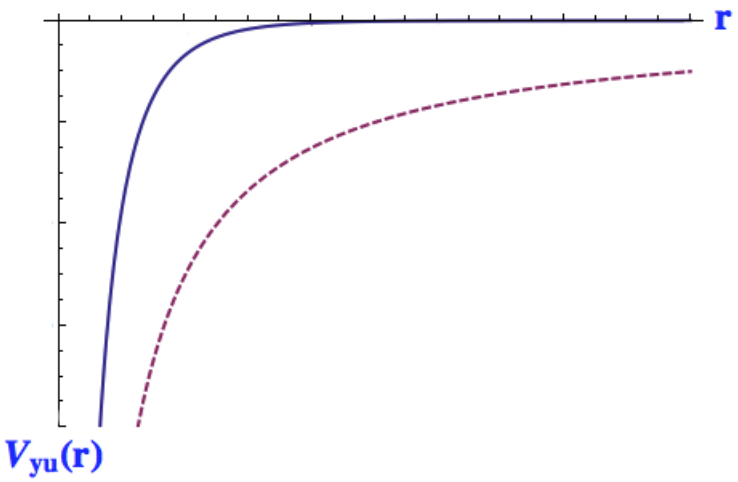

Figure 3.4: Two values of μ in the Yukawa potential, where the blue curve has μ value larger than 0, and the dashed curve has μ equals to 0 which turns to the Coulomb potential. We see the finite range of the Yukawa potential, and the infinite range of the Coulomb potential.

In order to use the numerical matrix method explained in Ch.2, we have to find the matrix elements of this potential from Eq.(2.11). For $l = 0$, we find the matrix elements of the Yukawa potential as

$$\mathbf{H_{nm}} = \delta_{nm} \left(\frac{\pi^2 n^2}{Ub^2} \right) - \frac{A}{b} \int_0^b \frac{\left[1 - \cos\left(\frac{\pi n r}{b}\right)\right] e^{-\mu r}}{r} \, dr. \tag{3.67}$$

Before we progress any further with a numerical calculation, let us try to have an idea about what

some of the estimating methods can tell us. In order to do so, let us firstly apply the B-S bound Eq.(1.19) to this potential. We find

$$N < \frac{UA}{\mu}. \tag{3.68}$$

Also, let us apply the C-C upper limit Eq.(1.24); we will find

$$N < 2\sqrt{\frac{2UA}{\pi\mu}}. \tag{3.69}$$

Both equations suggested that the FNE of this potential is $\frac{AU}{\mu}$. Accordingly, for now, we are going to assume this value to be the FNE. Then, to make sure our choice is right, we are going to test it with the numerical estimate, but before doing that we wish to normalize the energies to the Coulomb energies as (The Coulomb energies are written with general A and in units of U; for more details see Sec.(4.2) in Ch.4):

$$\epsilon = \frac{E}{E_0} = \frac{4E}{UA^2}; \qquad \beta = \frac{b}{a_0} = \frac{bUA}{2}, \tag{3.70}$$

where b is the size of the infinite wall in the matrix method. Then, by running the programme to test the assumed FNE, we find

U	μ	A	$\mathbf{G_{sug}} = AU/\mu$	ϵ_1	ϵ_2	β	n_{max}	N
1	1	1	1	−0.0205471	− − −−	100	1000	1
1	0.5	0.5	1	-0.0205471	− − −−	100	1000	1
1	0.25	0.25	1	−0.0205471	− − −−	100	1000	1
1	3	3	1	−0.0205471	− − −−	100	1000	1
1	0.1	0.1	1	−0.0205471	− − −−	100	1000	1
1	1	5	5	−0.653517	−0.0242094	50	500	2
1	2	10	5	−0.653517	−0.0242094	50	500	2
1	0.5	2.5	5	−0.653517	−0.0242094	50	500	2
1	0.1	0.5	5	−0.653517	−0.0242094	50	500	2

Table 3.1: A test of the suggested FNE $\mathbf{G_{sug}}$ of the Yukawa potential by the numerical matrix method. It is clear that this FNE is correct since we have fixed the value of FNE, and changed all its parameters, then we always found a fixed NBSE. The test has been carried out for two values of $\mathbf{G_{sug}}$: 1 and 5. Also, from the table we find that the values of ϵ are always the same when the value of FNE is fixed.

from Table 3.1 that FNE for this potential is

$$\mathbf{G_{yu}} = \frac{UA}{\mu}. \tag{3.71}$$

Now, let us turn to determining the critical point $\mathbf{G^c_{yu}}$ of this potential. To do that we have to use a similar procedure to the first example in Ch.2 (the finite spherical potential). We have to vary the size of the infinite wall b with the critical point of this potential until we can reach the asymptotic behaviour when $b \to \infty$. We found

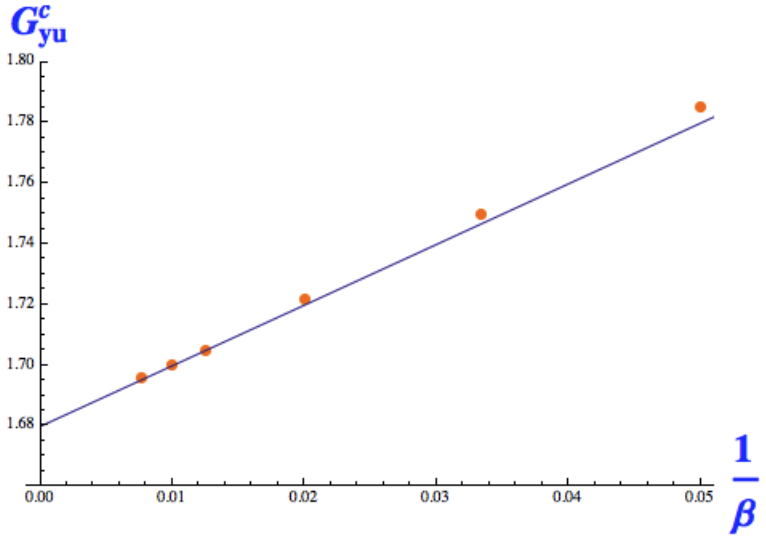

Figure 3.5: The critical point of the Yukawa potential. We find the exact critical point when the blue line intersects with the critcal point ($\mathbf{G^c_{yu}}(\beta)$) since this point corresponds to $b \to \infty$ where the effects of the infinite wall disappear. The exact value is $1.67983\cdots$

$$\mathbf{G^c_{yu}} = 1.67983\cdots . \tag{3.72}$$

This value agrees with [6], [36] [30]. Then, in order to test the efficiency of the estimating methods for this potential, let us apply the three necessary conditions Eqs.(3.14, 3.15, 3.16). We find

$$\begin{aligned} 1 &\leq \mathbf{G^c_{yu}}; \qquad \mathbf{G^c_{yu}} = 1, \\ 1 &\leq \mathbf{G^c_{yu}}^2(\ln(4) - 1); \qquad \mathbf{G^c_{yu}} = 1.60894, \\ 1 &\leq \mathbf{G^c_{yu}}^3\left(\tfrac{2}{3} - 3\ln(3) + \ln(16)\right); \qquad \mathbf{G^c_{yu}} = 1.66892. \end{aligned} \tag{3.73}$$

We find that they give very high accuracy; for example, the third one has 99% accuracy.

The upper and lower limits of this potential can be obtained from Eqs.(3.17), (3.18). They give

$$
\begin{aligned}
N &< \sqrt{\tfrac{2\mathbf{G_{yu}}}{\pi}} + \tfrac{1}{4\pi}\ln\left[\frac{\exp[-2\mathrm{Erf}^{-1}(h)^2+\mathrm{Erfc}^{-1}(h)^2]\mathrm{Erfc}^{-1}(h)^2}{\mathrm{Erf}^{-1}(h)^2}\right] + \tfrac{1}{2};\\
N &> \sqrt{\tfrac{2\mathbf{G_{yu}}}{\pi}} - \tfrac{1}{4\pi}\ln\left[\frac{\exp[-2\mathrm{Erf}^{-1}(h)^2+\mathrm{Erfc}^{-1}(h)^2]\mathrm{Erfc}^{-1}(h)^2}{\mathrm{Erf}^{-1}(h)^2}\right] - \tfrac{3}{2},
\end{aligned}
\tag{3.74}
$$

where Erf^{-1} is the inverse error function, Erfc^{-1} is the inverse complementary error function, and h is $\frac{1}{2}\sqrt{\frac{\pi}{2\mathbf{G_{yu}}}}$. We found the exact results are in the middle of the upper and lower limits, which indicates the upper and lower limits which are obtained from Eqs.(3.17, 3.18) are valid for the Yukawa potential.

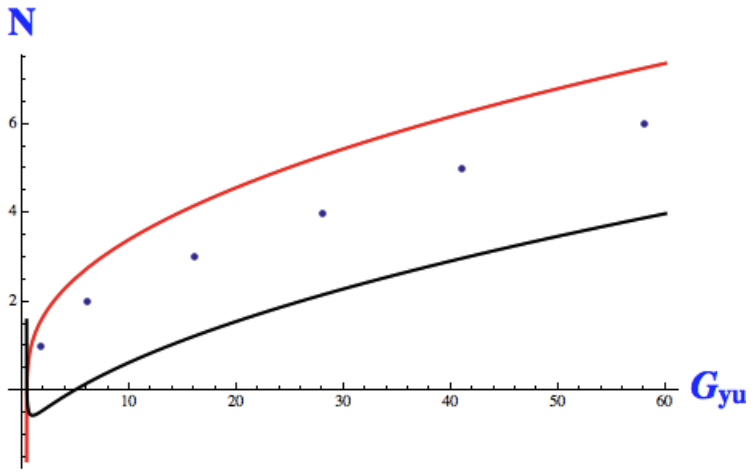

Figure 3.6: NBSE (N) in the Yukawa potential vs its FNE ($\mathbf{G_{yu}}$). The exact results of critical NBSE are the blue dots, the red curve shows the upper limit, and the black curve shows the lower limit of the Yukawa potential. However, we find the exact results are in between the two limits. Notice that the divergence at the origin does not have any physical meaning.

3.3 Three-parameter potentials

There are many examples in physics of potentials that have three parameters. These potentials are more general than the two-parameter potentials and they have different properties. One of these properties is that their FNE is usually more complicated than the two-parameter potentials; also, the FNE in these potentials is difficult to determine since it is not easy sometimes to find the exact N from the energy equation, as we will find with the cutoff triangular potential. Therefore, it is easier to study them by using the critical curve Def.(3) on page 20. The critical curve simplifies the analysis. Furthermore, when we fix the FNE in these potentials, we as usual will get the same

NBSE, but not the same eigenvalues as in two-parameter potentials.

In this section we will provide the FNE of each example and we will verify them with a table of results. Also, we will provide the exact critical curve and compare it with some of the estimating methods. Moreover, we will give the upper and lower limits for each potential without comparing them with the exact NBSE because three parameters need more than one curve to clarify and that is hard to represent, and that is not the focus of this study. The potentials that we are going to study are the finite spherical potential shell, the cutoff triangular potential and the Woods-Saxon potential.

3.3.1 Finite spherical potential shell

The finite spherical potential shell is a more general potential of the spherical potential. Also, this potential is the only non-monotonic potential in this thesis. This potential starts from a finite radius R and a thickness R_0, it has the definition

$$V_{shell}(r) = \begin{cases} 0 & \text{if } 0 < r < R; \\ -V_0 & \text{if } R < r < R + R_0; \\ 0 & \text{otherwise,} \end{cases} \tag{3.75}$$

Let us solve this potential by starting with the first region **I** from Figure 3.7. SE of this region is:

$$\frac{1}{U}\frac{d^2\chi_1}{dr^2} + E\chi_1 = 0, \tag{3.76}$$

the solution of this DE is

$$\chi_1 = b_1 e^{-kr} + b_2 e^{kr}, \qquad k = \sqrt{-UE}, \tag{3.77}$$

and its radial function is given by

$$\psi_1(r) = \frac{b_1 e^{-kr} + b_2 e^{kr}}{r}. \tag{3.78}$$

Then, its derivative is

$$\psi_1'(r) = -\frac{b_1 e^{-kr} + b_2 e^{kr}}{r^2} + k\frac{-b_1 e^{-kr} + b_2 e^{kr}}{r}. \tag{3.79}$$

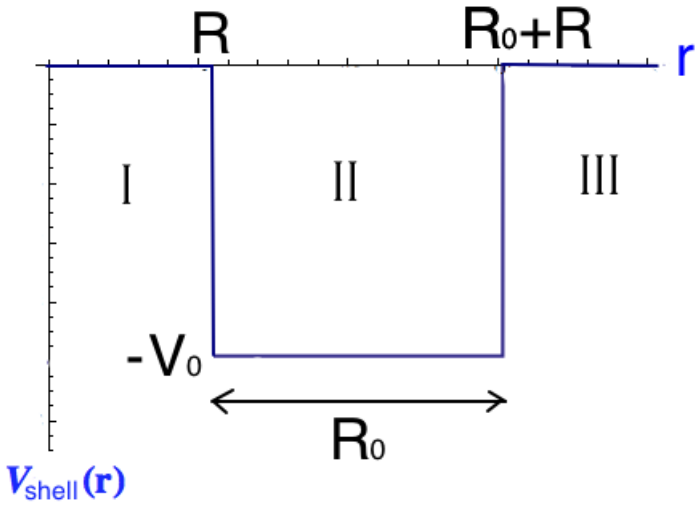

Figure 3.7: The spherical potential shell, where **I** is the first region, **II** is the second region, and **III** is the third region. V_0 is the depth of the potential, R is the additional radius and R_0 is the thickness of the shell

By dividing Eq.(3.79) over Eq.(3.78) we obtain

$$\frac{\psi_1'(r)}{\psi_1(r)} = -\frac{1}{r} + k\frac{A - e^{-2kr}}{A + e^{-2kr}}, \tag{3.80}$$

where A is b_2/b_1. The second region **II** has the SE

$$\frac{1}{U}\frac{d^2\chi_2}{dr^2} + [E + V_0]\,\chi_2 = 0, \tag{3.81}$$

and its solution is

$$\psi_2(r) = \frac{a_1\sin(qr) + a_2\cos(qr)}{r}, \qquad q = \sqrt{U(E+V_0)}. \tag{3.82}$$

Then, its derivative is

$$\psi_2'(r) = -\frac{a_1\sin(qr) + a_2\cos(qr)}{r^2} + q\frac{a_1\cos(qr) - a_2\sin(qr)}{r}. \tag{3.83}$$

By dividing $\psi_2'(r)$ and $\psi_2(r)$ and rearranging the results, we find

$$\frac{\psi_2'(r)}{\psi_2(r)} = -\frac{1}{r} + q\frac{B\cot(qr) - 1}{B + \cot(qr)}, \tag{3.84}$$

where B is a_1/a_2. The third region **III** has exactly the same solution of Eq.(3.35), we can write

$$\frac{\psi_3'(r)}{\psi_3(r)} = -k - \frac{1}{r}, \qquad k = \sqrt{-UE}. \tag{3.85}$$

Let us define $k/q = \omega$, and $q(R + R_0) = \phi$, and then apply the first continuity condition from Eqs.(3.84, 3.85) at $R + R_0$. After arranging the terms, we find

$$B\left(\omega + \cot(\phi)\right) = 1 - \omega\cot(\phi). \tag{3.86}$$

Then, by applying the second continuity condition from Eqs.(3.80, 3.84) at R, and substituting $kR = \theta$, and $qR = \phi_i$, we find by rearranging the result

$$B\left(\omega A - \omega e^{-2\theta} - \cot(\phi_i)e^{-2\theta} - A\cot(\phi_i)\right) = -e^{-2\theta} - A - \omega A\cot(\phi_i) + \omega e^{-2\theta}\cot(\phi_i). \tag{3.87}$$

To remove the parameter B, we can divide Eq.(3.87) by Eq.(3.86). After some manipulation, we obtain

$$Ae^{2\theta} = \frac{\omega^2[\cot(\phi_i) - \cot(\phi)] + [\cot(\phi_i) - \cot(\phi)]}{\omega^2[\cot(\phi_i) - \cot(\phi)] + 2w[1 + \cot(\phi_i)\cot(\phi)] - [\cot(\phi_i) - \cot(\phi)]}. \tag{3.88}$$

By using the trigonometric identity,

$$\cot(Q - Y) = \frac{1 + \cot(Q)\cot(Y)}{\cot(Y) - \cot(Q)}, \tag{3.89}$$

Eq. (3.88) reduces to

$$Ae^{2\theta}[\omega^2 + 2\omega\cot(\phi - \phi_i) - 1] = \omega^2 + 1, \tag{3.90}$$

which can be written as

$$\cot(\phi - \phi_i) = -\frac{\omega}{2}\left(1 - \frac{e^{-2\theta}}{A}\right) + \frac{1}{2\omega}\left(\frac{e^{-2\theta}}{A} + 1\right). \tag{3.91}$$

For $R \to 0$, we expect this equation to be that of the finite spherical potential. Indeed, we find

$$\cot(\phi) = -\frac{\omega}{2}\left(1 - \frac{1}{A}\right) + \frac{1}{2\omega}\left(\frac{1}{A} + 1\right). \tag{3.92}$$

If we put A equal to -1, Eq.(3.92) becomes:

$$\cot(\phi) = -\omega. \tag{3.93}$$

This equation is exactly what we have found with the finite spherical potential, and means that A should be equal to -1. Then, the finite spherical potential shell has the equation for the energy given by

$$\cot(\Phi) = -\frac{\omega}{2}\left(1 + e^{-2\theta}\right) + \frac{1}{2\omega}\left(1 - e^{-2\theta}\right), \tag{3.94}$$

where

$$\begin{aligned} \epsilon &= \tfrac{E}{V_0}; \\ \omega &= \sqrt{\tfrac{-\epsilon}{\epsilon+1}}; \\ \phi &= \sqrt{UV_0\left(R+R_0\right)^2(1+\epsilon)}; \\ \phi_i &= \sqrt{UV_0R^2(1+\epsilon)}; \\ \theta &= \sqrt{-UV_0R^2\epsilon}; \\ \Phi = \phi - \phi_i &= \sqrt{UV_0R_0^2(1+\epsilon)}. \end{aligned} \tag{3.95}$$

When $R \to \infty$, we obtain

$$\cot(\Phi) = \sqrt{\frac{\epsilon^2 + \epsilon + \frac{1}{4}}{-\epsilon^2 - \epsilon}}. \tag{3.96}$$

The energy equation for this potential is given by Eq.(3.94), which means that in order to find the value of the normalized energy ϵ, we have to plot the LHS and the RHS of this equation with respect to ϵ in the same plot. The intersection points indicate the value of ϵ_n. The FNE of this potential is obtained from the equation of energy for this potential by putting $\epsilon \to 0$,

$$\cot\left(\sqrt{UV_0R_0^2}\right) = \frac{1}{2}\lim_{\epsilon\to 0}\sqrt{\frac{\epsilon+1}{-\epsilon}}\left(1 - e^{-2\sqrt{-UV_0R^2\epsilon}}\right). \tag{3.97}$$

Using the Taylor series of the exponential term,

$$e^{-2\sqrt{-UV_0R^2\epsilon}} = 1 + 2\sqrt{-UV_0R^2\epsilon} + \cdots, \tag{3.98}$$

we get

$$\sqrt{UV_0R_0^2} - \cot^{-1}\left(\sqrt{UV_0R^2}\right) = 0. \tag{3.99}$$

We define from the previous equation the FNS of this potential as

$$\mathbf{G_{shell}} = \sqrt{UV_0R_0^2} - \cot^{-1}\left(\sqrt{UV_0R^2}\right), \tag{3.100}$$

with critical point equals to 0. Now, let us test this FNE with the Table 3.2. It shows some values of

U	V_0	R_0	R	$\mathbf{G_{shell}}$	ϵ_1	N
2	1	2	0	1.25763	−0.377201	1
2	1	1.9	0.100672	1.25763	−0.377201	1
2	1	1.3	1.07728	1.25763	−0.368262	1
2	1	0.9	46.635	1.25763	−0.189866	1
2	1	8	0	9.74291	−0.0269194	4
1	2	7.7	0.319398	9.74291	−0.0269165	4
1	2	7.2	1.50423	9.74291	−0.0263142	4
1	2	6.89	693.746	9.74291	−0.0150177	4

Table 3.2: Verification of the FNE for the finite spherical potential shell Eq.(3.100) for two values of $\mathbf{G_{shell}}$, 1.25763, and 9.74291. This FNE is really fixing NBSE which appear in the table in the column N.

the exact expression of the FNE. Also, from Eq.(3.100) we can say that the NBSE of this potential for a given value of $(UV_0R_0^2)$ is always the same NBSE as for the finite spherical potential or one more bound state.

Now, let us find the analytical critical curve $\mathbf{W_c}$ for this potential. We define the following

$$\mathbf{W_c} = UV_0R_0^2; \qquad \mathbf{g} = UV_0R^2. \tag{3.101}$$

Let us call this representation the **g**-representation. Then, Eq.(3.99) is rewritten as

$$\mathbf{W_c} = \left[\cot^{-1}\left(\sqrt{\mathbf{g}}\right)\right]^2. \tag{3.102}$$

Each point from the above expression represents a trivial critical point see Figure 3.8. Also, any point above this curve will admit a bound state, and below this curve there will be no bound state at all.

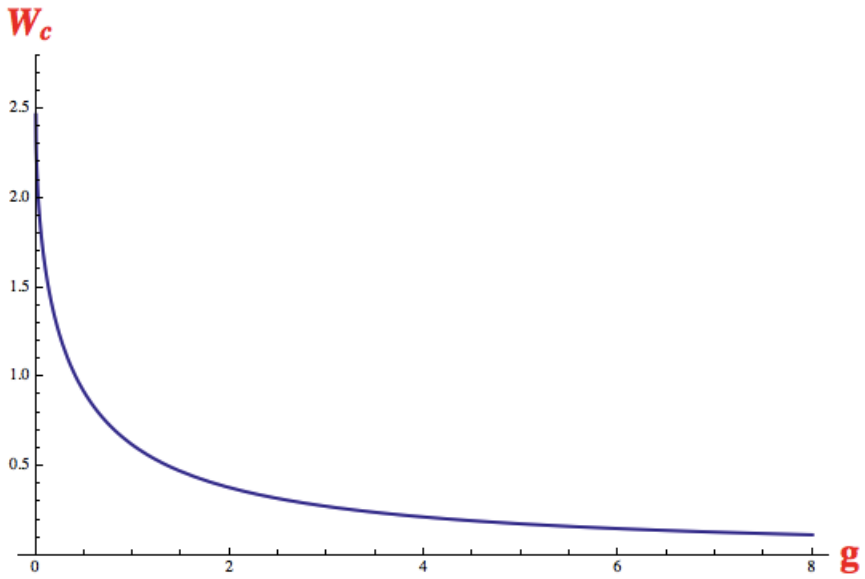

Figure 3.8: The critical curve of the spherical potential shell Eq.(3.102) with **g**-rep. Notice that when $\mathbf{g} \to 0$, it gives the same value as the finite spherical potential which is $\pi^2/4$.

Next, let us find the critical curve from the estimating methods for the Eqs.(3.14, 3.15, 3.16). However, it is difficult to plot them in the **g**-representation (or **g**-rep.). Accordingly, we will use another representation which I called the **f**-representation (or **f**-rep.), where f is defined as R/R_0 (see Figure 3.9). For this representation, Eq.(3.102) becomes

$$\mathbf{W_c} = \left[\cot^{-1}\left(\sqrt{\mathbf{W_c} f^2}\right)\right]^2. \tag{3.103}$$

Then, the three estimating methods respectively give

$$\begin{aligned} W_c &= \tfrac{1}{f+0.5}; \\ W_c &= \tfrac{1}{\sqrt{f^2+\frac{2}{3}f+\frac{1}{6}}}; \\ W_c &= \tfrac{1}{\left(f^3+f^2+\frac{2}{5}f+\frac{1}{15}\right)^{1/3}}. \end{aligned} \tag{3.104}$$

Finally, we cannot apply the upper and lower limits to this potential since it is a non-monotonic potential. However, the NBSE of this potential is always the same NBSE as the finite spherical

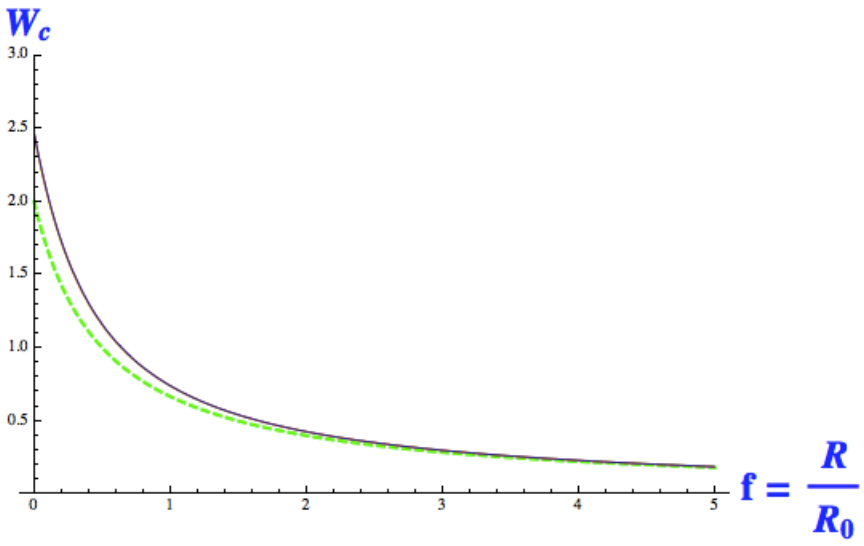

Figure 3.9: The critical curve of the spherical potential shell Eq.(3.103) with **f**-rep (blue curve behind the pink curve), the yellow curve is Eq.(3.15), and the pink curve is Eq.(3.16). All these curves are close to each other. The green dashed curve is Eq.(3.14). The second and third approximations give high accuracy.

potential or one more bound state energy.

3.3.2 Cutoff triangular potential

This potential is a simplified form of the Woods-Saxon potential which is sometimes called the first moment of the Woods-Saxon potential. It involves performing a cutoff to the triangular potential, the cutoff being just the finite spherical potential. The cutoff triangular potential has this definition

$$V_{ctri}(r) = \begin{cases} -V_0 & \text{if } 0 < r < R_0; \\ -V_0 \left[1 - \frac{r-R_0}{a}\right] & \text{if } R_0 < r < R_0 + a; \\ 0 & \text{otherwise,} \end{cases} \tag{3.105}$$

which if we make $R_0 \to 0$, becomes the triangular potential, and if $a \to 0$, it gives the finite spherical potential.

Let us start by solving SE for the first region **I** in Figure 3.10. This region is already solved in

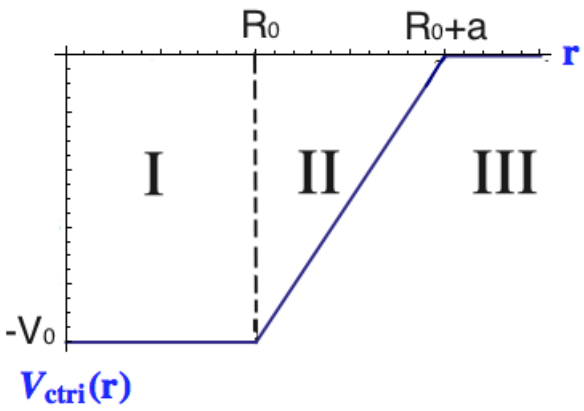

Figure 3.10: The cutoff triangular potential, where **I** is the first region, **II** is the second region, and **III** is the third region.

the spherical potential section Eq.(3.30), and the result is

$$\frac{\psi_1'(r)}{\psi_1(r)} = q\cot(qr) - \frac{1}{r}; \qquad q = \sqrt{U(E+V_0)}. \tag{3.106}$$

Then, the second region **II** has the following SE

$$\frac{1}{U}\frac{d^2\chi_2}{dr^2} + \left[E + V_0\left(1 - \frac{r-R_0}{a}\right)\right]\chi_2 = 0, \tag{3.107}$$

which is rewritten as

$$-\frac{1}{U}\frac{d^2\chi_2}{dr^2} + \frac{rV_0}{a}\chi_2 = \left(E + V_0 + \frac{R_0V_0}{a}\right)\chi_2. \tag{3.108}$$

By changing the variables we find

$$r = \rho_c y + \sigma_c, \tag{3.109}$$

where

$$\rho_c = \left(\frac{a}{UV_0}\right)^{1/3}, \qquad \sigma_c = \frac{(E + V_0 + \frac{R_0V_0}{a})a}{V_0} = \left[1 + \epsilon + \frac{R_0}{a}\right]a, \tag{3.110}$$

where ϵ is E/V_0, then Eq.(3.108) becomes

$$\frac{d^2\chi_2}{dy^2} = y\chi_2, \tag{3.111}$$

the solution of this DE has been found for the triangular potential Eq.(3.54), and the final solution is

$$\frac{\psi_2'(r)}{\psi_2(r)} = \frac{CAi'\left(\frac{r-\sigma_c}{\rho_c}\right) + Bi'\left(\frac{r-\sigma_c}{\rho_c}\right)}{\rho_c\left[CAi\left(\frac{r-\sigma_c}{\rho_c}\right) + Bi\left(\frac{r-\sigma_c}{\rho_c}\right)\right]} - \frac{1}{r}. \tag{3.112}$$

Also, in the third region **III**, the solution has been obtained for the spherical potential Eq.(3.35). Then its final result is

$$\frac{\psi_3'(r)}{\psi_3(r)} = -k - \frac{1}{r}; \qquad k = \sqrt{-UE}. \tag{3.113}$$

Then, let us apply the continuity conditions. First of all between regions **II** and **III** at $R_0 + a$, we find

$$\frac{CAi'\left(\frac{(R_0+a)-\sigma_c}{\rho_c}\right) + Bi'\left(\frac{(R_0+a)-\sigma_c}{\rho_c}\right)}{\rho_c\left[CAi\left(\frac{(R_0+a)-\sigma_c}{\rho_c}\right) + Bi\left(\frac{(R_0+a)-\sigma_c}{\rho_c}\right)\right]} = -k. \tag{3.114}$$

By defining $\frac{R_0+a-\sigma_c}{\rho_c} \equiv -\Theta\epsilon$, where $\Theta = a/\rho_c$, and $\rho_c k \equiv \sqrt{-\epsilon\Theta}$, Eq.(3.114) becomes

$$\frac{CAi'\left(-\Theta\epsilon\right) + Bi'\left(-\Theta\epsilon\right)}{CAi\left(-\Theta\epsilon\right) + Bi\left(-\Theta\epsilon\right)} = -\sqrt{-\epsilon\Theta}. \tag{3.115}$$

Then, we apply the second continuity conditions between regions **I** and **II** at $r = R_0$. Before that, let us define $\frac{R_0-\sigma_c}{\rho_c} \equiv -\Theta(1+\epsilon)$, and $\rho_c q \equiv \sqrt{\Theta(1+\epsilon)}$, and finally $qR_0 \equiv \Phi$. Therefore, we will end up with

$$\frac{CAi'\left(-\Theta(1+\epsilon)\right) + Bi'\left(-\Theta(1+\epsilon)\right)}{CAi\left(-\Theta(1+\epsilon)\right) + Bi\left(-\Theta(1+\epsilon)\right)} = \sqrt{\Theta(1+\epsilon)}\cot(\Phi). \tag{3.116}$$

Now, let us combine both continuity conditions in order to get rid of C, we find

$$\cot(\Phi) = \frac{Bi'(-\Theta(1+\epsilon)) - Ai'(-\Theta(1+\epsilon))\frac{Bi'(-\Theta\epsilon)+\sqrt{-\Theta\epsilon}Bi(-\Theta\epsilon)}{Ai'(-\Theta\epsilon)+\sqrt{-\Theta\epsilon}Ai(-\Theta\epsilon)}}{\sqrt{\Theta(1+\epsilon)}\left[Bi(-\Theta(1+\epsilon)) - Ai(-\Theta(1+\epsilon))\frac{Bi'(-\Theta\epsilon)+\sqrt{-\Theta\epsilon}Bi(-\Theta\epsilon)}{Ai'(-\Theta\epsilon)+\sqrt{-\Theta\epsilon}Ai(-\Theta\epsilon)}\right]} \tag{3.117}$$

where

$$\begin{aligned} \Theta &= (UV_0a^2)^{1/3}; \\ \Phi &= \sqrt{UV_0R_0^2(1+\epsilon)}. \end{aligned} \tag{3.118}$$

Now, let us make sure that Eq.(3.117) covers both limits of spherical and triangular potentials. In the limit $R_0 \to 0$ we expect this equation to cover the energy equation of the triangular potential, and we find

$$\frac{Ai(-(1+\epsilon)\Theta)\left[Bi'(-\Theta\epsilon) + \sqrt{-\Theta\epsilon}Bi(-\Theta\epsilon)\right]}{Bi(-(1+\epsilon)\Theta)\left[Ai'(-\Theta\epsilon) + \sqrt{-\Theta\epsilon}Ai(-\Theta\epsilon)\right]} = 1. \tag{3.119}$$

This is exactly the same equation for energy as for the triangular potential. Then, the second limit is $a \to 0$ or $\Theta \to 0$, and we expect the energy equation to be the same as for the spherical potential energy equation. Therefore, if we take the limit $\Theta \to 0$ on the RHS of Eq.(3.117), we find

$$\cot(\Phi) = -\sqrt{\frac{-\epsilon}{\epsilon+1}}, \tag{3.120}$$

where this is the exact energy equation of the regular spherical potential. Now, let us find the limit $\epsilon \to 0$, then we obtain

$$\cot\left[\sqrt{UV_0R_0^2}\right] = \frac{\sqrt{3}Ai'(-\Theta) + Bi'(-\Theta)}{\sqrt{\Theta}\left(\sqrt{3}Ai(-\Theta) + Bi(-\Theta)\right)}. \tag{3.121}$$

Since the LHS and the RHS of the previous equation have an infinite number of zeros, determining the general FNE is really difficult. If we want to do so, we have to specify a range for each value of NBSE N. However, one of the FNE formulas of this potential can be written as

$$\mathbf{G_{ctri}} = \sqrt{UV_0R_0^2} - \cot^{-1}\left[\frac{\sqrt{3}Ai'(-\Theta) + Bi'(-\Theta)}{\sqrt{\Theta}\left(\sqrt{3}Ai(-\Theta) + Bi(-\Theta)\right)}\right]. \tag{3.122}$$

Also, we can write the FNE with other formulas. However, the differences between one FNE and another is the range and the complexity. We find it difficult to determine the full FNE from Eq.(3.121) since we cannot find the exact expression of N from that equation. However, Eq.(3.122) is sufficient to represent some properties of FNE of this potential.

U	V_0	R_0	a	$\mathbf{G_{ctri}}$	ϵ_1	N
2	1	1	1	0.573999	−0.131169	1
2	1	0.392231	2	0.573999	−0.0822572	1
2	1	0.117167	2.4	0.573999	−0.0664018	1
2	1	0.0466923	2.5	0.573999	−0.0664018	1
2	1	6	1	7.64507	−0.178089	3
1	2	5.39223	2	7.64507	−0.148908	3
1	2	5.04669	2.5	7.64507	−0.131963	3
1	2	5.00423	2.56	7.64507	−0.130122	3

Table 3.3: Verification of the FNE for the cutoff triangular potential Eq.(3.122) for two values of $\mathbf{G_{ctri}}$, 0.573999, and 7.64507. This FNE is fixing NBSE as it appears in the table in the final column N.

Then, we find the critical curve in **g**-rep as

$$\mathbf{W_c} = \left[\cot^{-1}\left(\frac{Bi'(-\mathbf{g}^{1/3}) + \sqrt{3}Ai'(-\mathbf{g}^{1/3})}{\mathbf{g}^{1/6}[Bi(-\mathbf{g}^{1/3}) + \sqrt{3}Ai(-\mathbf{g}^{1/3})]}\right)\right]^2, \tag{3.123}$$

where $\mathbf{g}$ is UV_0a^2, and $\mathbf{W_c}$ is $UV_0R_0^2$. Again, this function has an infinite number of zeros. Since our interest is in the existence of the first bound state, we will plot it just for the first zero, Figure 3.11.

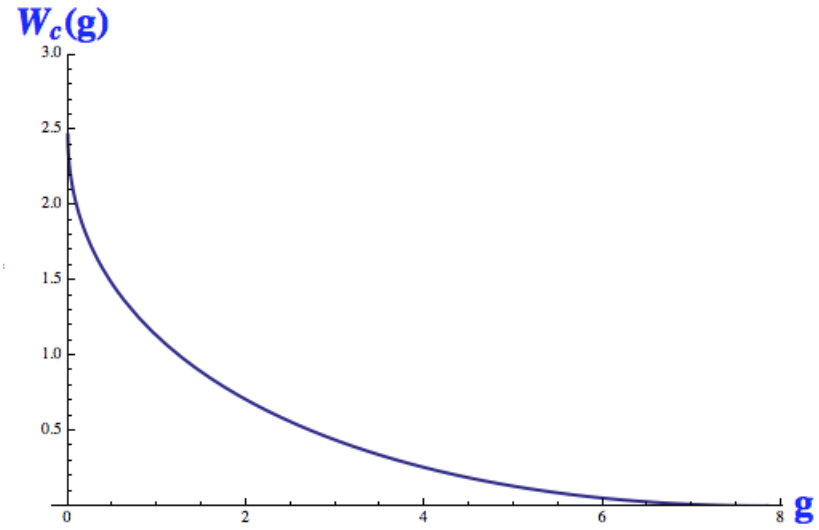

Figure 3.11: The critical curve of the cutoff triangular potential in **g**-rep. Each point of this curve represents a trivial critical point. Also, we find that the curve intersects with y-axis in the critical point of the finite spherical potential ($\mathbf{G^c_{sph}}$), and intersects with x-axis in the critical point of the triangular potential ($\mathbf{G^c_{tri}}$) .

Next, let us find the critical curve by using some of the estimating methods. These methods are the necessary conditions. The results appear by the **f**-rep, which defined as $f = a/R_0$.

$$\begin{aligned}
\mathbf{W_c} &= \tfrac{2}{\frac{f^2}{3}+f+1}; \qquad Eq.(3.14),\\
\mathbf{W_c}^2 &= \tfrac{1}{\frac{f^4}{30}+\frac{f^3}{6}+\frac{f^2}{3}+\frac{f}{3}+\frac{1}{6}}; \quad Eq.(3.15),\\
\mathbf{W_c}^3 &= \tfrac{1}{\frac{f^6}{105}+\frac{f^5}{15}+\frac{3f^4}{5}+\frac{f^3}{3}+\frac{f^2}{3}+\frac{f}{5}+\frac{1}{15}} \quad Eq.(3.16).
\end{aligned} \tag{3.124}$$

These results are obtained by considering $r_1 < R_0$ and $r_2 < R_0$, that is why the plots in Figure 3.12 have accurate points when $f \to 0$, but have a weak accuracy when $f \to \infty$. If we want to have a

high accuracy in the opposite limit, we have to change the assumption in r_1 and r_2 to $r_1 > R_0$ and $r_2 > R_0$.

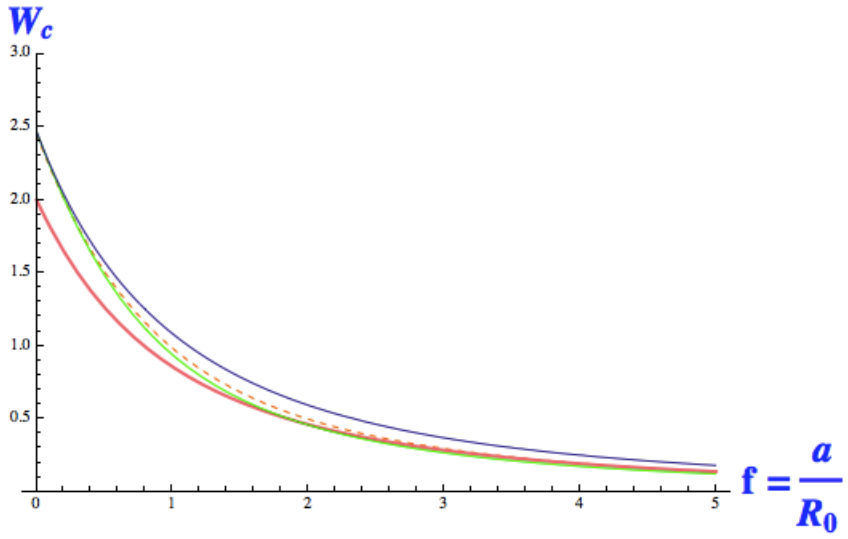

Figure 3.12: The exact critical curve of the cutoff triangular potential in **f**-rep (blue curve), Eq.(3.14) is the thick pink curve, Eq.(3.15) is the orange dashed curve, and Eq.(3.16) is the green curve below the dashed curve. We find the high accuracy results when $f \to 0$.

We can find the upper and lower limits for this potential by using Eqs.(3.17, 3.18). By omitting the value of p and q, we find

$$\begin{aligned} N &< \tfrac{\sqrt{UV_0}}{3\pi}(2a + 3R_0) + \tfrac{1}{2}, \\ N &> \tfrac{\sqrt{UV_0}}{3\pi}(2a + 3R_0) - \tfrac{3}{2}. \end{aligned} \tag{3.125}$$

3.3.3 Woods-Saxon potential

The Woods-Saxon potential is one of the important physical potentials in nuclear physics to describe the strong force of the nucleus. However, this potential cannot be solved exactly in SE for a general value of l. Therefore, only for the case $l = 0$ it has been solved exactly, and approximation methods have been used to solve it in the general case [34], [37]. The equation of energy for $l = 0$ is given by Flügge [38]. He used some properties of the hypergeometric functions in order to solve SE. However, we just provide the expression here without giving the detailed steps. The Woods-Saxon potential

is described by

$$V_{ws} = \frac{-V_0}{1 + \exp\left(\frac{r-R_0}{a}\right)}, \tag{3.126}$$

and looks like Figure 3.13. As $a \to 0$, this expression turns into the finite spherical potential. Our

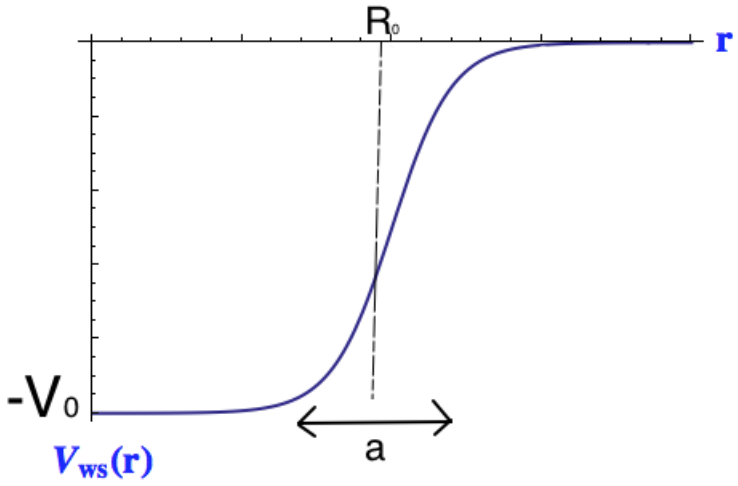

Figure 3.13: The Woods-Saxon potential with V_0 is the depth, R_0 is radius of the nucleus, and a is the surface thickness.

interest here is the physical range of a which is usually less than

$$f = \frac{a}{R_0} < 0.3. \tag{3.127}$$

Then, the final energy equation of this potential in the case $l = 0$ is

$$\frac{\chi}{k} = -cot\left[kR_0 - \sum_{n=1}^{\infty}\left(\tan^{-1}\left(\frac{2ka}{n}\right) - 2\tan^{-1}\left(\frac{ka}{n+\chi a}\right)\right)\right], \tag{3.128}$$

where

$$\chi = \sqrt{-UV_0\epsilon}\,;$$

$$k = \sqrt{UV_0(1+\epsilon)}\,,$$

where ϵ is E/V_0, and U is $2m/\hbar^2$. If we set $a \to 0$ in Eq.(3.128), it will become the energy equation of the finite spherical potential Eq.(3.37). Although this eigenvalue equation is exact, it just valid

when R_0 is much grater than a ($R_0 >> a$). For more details about this see [38]. Now, let us study the criteria for bound state energies of this potential by setting $\epsilon \to 0$; we find

$$0 = \cot\left[kR_0 - \sum_{n=1}^{\infty}\left(\tan^{-1}\left(\frac{2ka}{n}\right) - 2\tan^{-1}\left(\frac{ka}{n}\right)\right)\right], \tag{3.129}$$

which leads to

$$\left(N - \frac{1}{2}\right)\pi = kR_0 - \sum_{n=1}^{\infty}\left(\tan^{-1}\left(\frac{2ka}{n}\right) - 2\tan^{-1}\left(\frac{ka}{n}\right)\right), \tag{3.130}$$

and is rewritten as

$$N = \left[\frac{kR_0}{\pi} - \frac{1}{\pi}\sum_{n=1}^{\infty}\left(\tan^{-1}\left(\frac{2ka}{n}\right) - 2\tan^{-1}\left(\frac{ka}{n}\right)\right) + \frac{1}{2}\right], \tag{3.131}$$

where $[Q]$ means the nearest integer less than the value of Q. The previous equation is NBSE equation of Woods-Saxon potential. Also, from this equation we find that the FNE is written as

$$\mathbf{G_{W-S}} = kR_0 - \sum_{n=1}^{\infty}\left(\tan^{-1}\left(\frac{2ka}{n}\right) - 2\tan^{-1}\left(\frac{ka}{n}\right)\right). \tag{3.132}$$

The critical value of this potential is obviously

$$\mathbf{G^c_{W-S}} = \frac{\pi}{2}. \tag{3.133}$$

Then, to test this expression see Table 3.4. Then, we provide the critical curve in **g**-rep from

U	V_0	R_0	a	$\mathbf{G_{W-S}}$	ϵ_1	N
0.1	1	20	0	6.32456	-0.299892	2
0.1	1	19.9852	0.4	6.32456	-0.295	2
0.1	1	19.8546	0.9	6.32456	-0.27649	2
0.1	1	19.018	2	6.32456	-0.211927	2
0.1	3	9.9904	2	6.32456	-0.134689	2
1	0.05	50	0	11.1803	-0.0127604	4
0.1	1	35.1632	1	11.1803	-0.00983088	4
0.05	3	27.6695	2	11.1803	-0.0043716	4
5	0.04	21.0525	4	11.1803	-0.00103587	4

Table 3.4: Verification of the FNE for the Woods-Saxon potential Eq.(3.132) for two values of **G**, 6.32456, and 11.1803. This fixed number expression is really fixing NBSE which appear in the table in the column N.

Eq.(3.129) as

$$\mathbf{W_c} = \left[\frac{\pi}{2} + \sum_{n=1}^{\infty}\left(\tan^{-1}\left(\frac{2\sqrt{\mathbf{g}}}{n}\right) - 2\tan^{-1}\left(\frac{\sqrt{\mathbf{g}}}{n}\right)\right)\right]^2, \tag{3.134}$$

where $\mathbf{W_c}$ is $UV_0R_0^2$ and $\mathbf{g}$ is UV_0a^2 (see Figure 3.14).

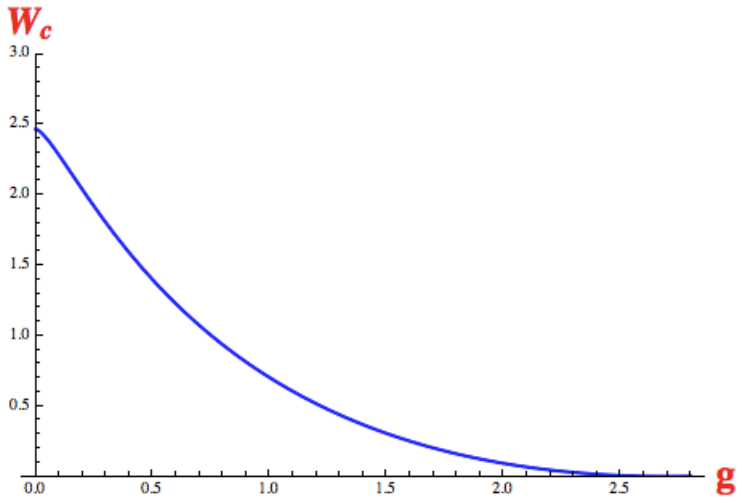

Figure 3.14: The critical curve of the Woods-Saxon potential in **g**-rep Eq.(3.134), we can see the intersection point in y-axis is the critical point of the finite spherical potential which is $\pi^2/4$.

Then, let us use some of the estimating methods for the critical curve. We will use just the first equation of the necessary condition, equations Eq.(3.14), since the integration of this potential is not easy to do. We will provide the results in **f**-rep see Figure 3.15.

$$\mathbf{W_c} = \frac{2}{1 + \frac{\pi^2 f^2}{3} + f^2 \mathrm{Li}_2\left(e^{-1/f}\right)}, \tag{3.135}$$

where f is a/R_0, and Li_2 is the polylogarithm function, which has the definition

$$\mathrm{Li}_2(x) = \sum_{k=1}^{\infty}\frac{x^k}{k^2}. \tag{3.136}$$

The exact critical curve in **f**-rep is obtained from Eq.(3.129) as

$$\mathbf{W_c} = \left[\frac{\pi}{2} + \sum_{n=1}^{\infty}\left(\tan^{-1}\left(\frac{2f\sqrt{\mathbf{W_c}}}{n}\right) - 2\tan^{-1}\left(\frac{f\sqrt{\mathbf{W_c}}}{n}\right)\right)\right]^2, \tag{3.137}$$

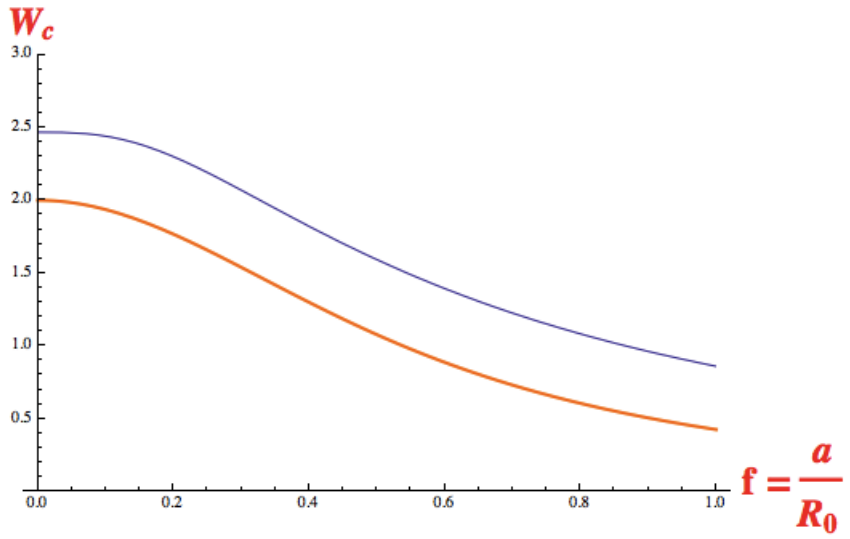

Figure 3.15: The exact critical curve of the Woods-Saxon potential in **f**-rep Eq.(3.137) (the blue curve which starts from $\pi^2/4$), and Eq.(3.135) is the orange curve.

Now, let us determine the upper and lower limits of this potential without considering p and q from Eqs.(3.17, 3.18),

$$\begin{aligned} N &< \sqrt{UV_0a^2}\left[1+\ln\left(\sqrt{1+e^{-1/f}}\right)-\ln\left(\sqrt{1+e^{-1/f}}-1\right)\right]+\tfrac{1}{2}; \\ N &> \sqrt{UV_0a^2}\left[1+\ln\left(\sqrt{1+e^{-1/f}}\right)-\ln\left(\sqrt{1+e^{-1/f}}-1\right)\right]-\tfrac{3}{2}. \end{aligned} \tag{3.138}$$

These equations are the upper and lower limits of Woods-Saxon potential, and their results are in agreement with the results of Table 3.4, if we add to Eq.(3.138) $[Q]$ as in Eq.(3.39).

Chapter 4

Infinite or finite number of bound state energies

In this chapter we study the condition for the presence of an infinite or finite number of bound state energies (NBSE) for a potential. There are a lot of potentials that have an infinite NBSE for the $3D$ SE in physics such as the Coulomb potential. Our main question is: are the estimating methods in Ch.1 able to predict whether a potential has an infinite or finite NBSE? We will answer this question by solving SE and comparing the results with some of the estimating methods.

We have organized this chapter as follows: the first section will discuss some general outline about solving SE. The second section is for solving the Coulomb potential. Then, the third section is for the cutoff Coulomb potential. The fourth section will discuss solving the cutoff inverse square potential. The final section is for solving the cutoff inverse cubic potential.

4.1 General outlines

The potentials having an infinite NBSE have some different criteria for bound state energies than the finite ones. For instance, the idea of the fixed number expression (FNE) is not present, the critical point or curve also does not exist. Therefore, our main concentration will be to determine whether a potential has an infinite or finite NBSE. This determination can be done, often graphically, when we find the energy equation (usually implicit) for a potential. Then, this equation tells us whether, for that potential there are a finite or infinite NBSE by analysis or by plotting the energy equation.

Moreover, we will give an idea about how the eigenvalues can be described by the principal quantum number n.

We found all estimating methods given in Ch.1 really provide estimates concerning the existence of infinite or finite NBSE, which means all the estimating methods are powerful in this sense. All potentials we consider in this chapter are with a short distance cutoff which we use the spherical well potential. Therefore, we will also provide a new estimating method of the NBSE for these potentials, which is the number of bound states expected by considering the spherical potential Eq.(3.39) alone,

$$N = \frac{1}{\pi}\sqrt{UR_0^2V_0} + \frac{1}{2}, \tag{4.1}$$

where $U = 2m/\hbar^2$, R_0 and V_0 are the range and the depth of the spherical potential respectively. Also, for an extreme cutoff (i.e. $UR_0^2V_0 >> \pi^2$), we can predict the value of the first few bound state energies from Eq.(3.43)

$$E_n = \frac{n^2\pi^2}{UR_0^2} - V_0. \tag{4.2}$$

We will be again applying the continuity conditions in this chapter, but here the entire region $r < R_0$ is described by the spherical potential expression which means we will use Eq.(3.30),

$$\frac{\psi_1'(r)}{\psi_1(r)} = q\cot(qr) - \frac{1}{r}; \qquad q = \sqrt{U(E+V_0)}. \tag{4.3}$$

For this region, this will be true for all potentials in this chapter except the cutoff cubic potential, where we will use the numerical method explained in Chapter 2.

4.2 Coulomb potential

The Coulomb potential is one of the important potentials in physics, and has several applications such as the hydrogen-like atom. This potential is solved analytically for any value of l by using various methods. The well-known fact about this potential is that it supports an infinite NBSE. In this section we will use the direct method to solve the SE using the hypergeometric functions for the case of $l = 0$. This potential is given as

$$V_{cou} = -\frac{A}{r}, \tag{4.4}$$

where A is the strength of the Coulomb potential. The potential is plotted in Figure 4.1. The radial

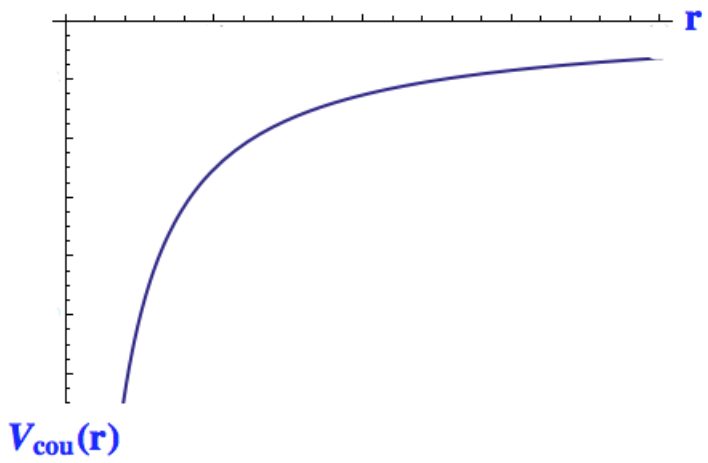

Figure 4.1: The Coulomb potential, with A is the strength.

Schrödinger equation for this potential is given as:

$$-\frac{1}{U}\frac{\partial^2\chi}{\partial r^2} - \frac{A}{r}\chi = E\chi, \tag{4.5}$$

or

$$\frac{\partial^2\chi}{\partial r^2} + \frac{UA}{r}\psi + UE\chi = 0. \tag{4.6}$$

Now, let us change the variables to:

$$x = \delta r; \qquad \text{with} \qquad \left(\frac{\delta}{2}\right)^2 = -UE, \tag{4.7}$$

then Eq.(4.6) becomes

$$\frac{\partial^2\chi}{\partial x^2} + \left[\frac{S}{x} - \frac{1}{4}\right]\chi = 0 \qquad \text{with} \qquad S = \frac{UA}{\delta} = \frac{UA}{\sqrt{-4UE}}. \tag{4.8}$$

Now we perform a transformation on χ

$$\chi = e^{-x/2}W(x). \tag{4.9}$$

Then, Eq.(4.8) becomes

$$\frac{d^2W}{dx^2} - \frac{dW}{dx} + \frac{S}{x}W = 0. \tag{4.10}$$

Using another transformation on W

$$W(x) = xQ(x), \tag{4.11}$$

leads to

$$x\frac{d^2Q}{dx^2} + (2-x)\frac{dQ}{dx} - (1-S)Q = 0. \tag{4.12}$$

The differential equation (DE) having the form of Eq.(4.12) is called Kummer's equation. It has this general form:

$$z\frac{d^2P}{dz^2} + (b-z)\frac{dP}{dz} - aP = 0, \tag{4.13}$$

and its general solution is:

$$P = B\,{}_1\mathbf{F_1}(a,b,z) + C\,\mathbf{U}(a,b,z), \tag{4.14}$$

where ${}_1\mathbf{F_1}$ and $\mathbf{U}$ are the confluent hypergeometric functions. They have many definitions, one of which is the series representation

$$\begin{aligned} {}_1\mathbf{F_1}(a,b,x) &= \textstyle\sum_{n=0}^{\infty} \frac{a^{(n)}x^n}{b^{(n)}n!}; \\ \mathbf{U}(a,b,x) &= \textstyle\frac{\Gamma(1-b)}{\Gamma(a-b+1)}{}_1\mathbf{F_1}(a,b,x) + \frac{\Gamma(b-1)}{\Gamma(a)}x^{1-b}\,{}_1\mathbf{F_1}(a-b+1,2-b,x), \end{aligned} \tag{4.15}$$

where $a^{(n)}$ is defined as

$$a^{(n)} = a(a+1)(a+2)\cdots(a+n-1) \qquad \text{with} \quad a^{(0)} = 1. \tag{4.16}$$

Now, by comparing Eq.(4.14) with Eq.(4.12), we find that $b = 2$, and $a = 1 - S$. Therefore, we write:

$$Q = B\,{}_1\mathbf{F_1}(1-S,2,x) + C\,\mathbf{U}(1-S,2,x). \tag{4.17}$$

Then, we can easily find the auxiliary radial wave function χ as

$$\chi(x) = e^{-x/2}x\Big[C_1\,{}_1\mathbf{F_1}(1-S,2,x) + C_2\,\mathbf{U}(1-S,2,x)\Big], \tag{4.18}$$

and the radial wave function ψ is found to be

$$\psi(r) = e^{-\frac{\delta}{2}r}\delta\Big[B\,{}_1\mathbf{F_1}(1-S,2,\delta r) + C\,\mathbf{U}(1-S,2,\delta r)\Big]. \tag{4.19}$$

Now, let us determine which term of these two terms can be a physical solution. First, let us draw a curve for both terms by giving S the value of an integer, say 2, and then lower and raise this value by a small value, to determine the behaviour of these functions.

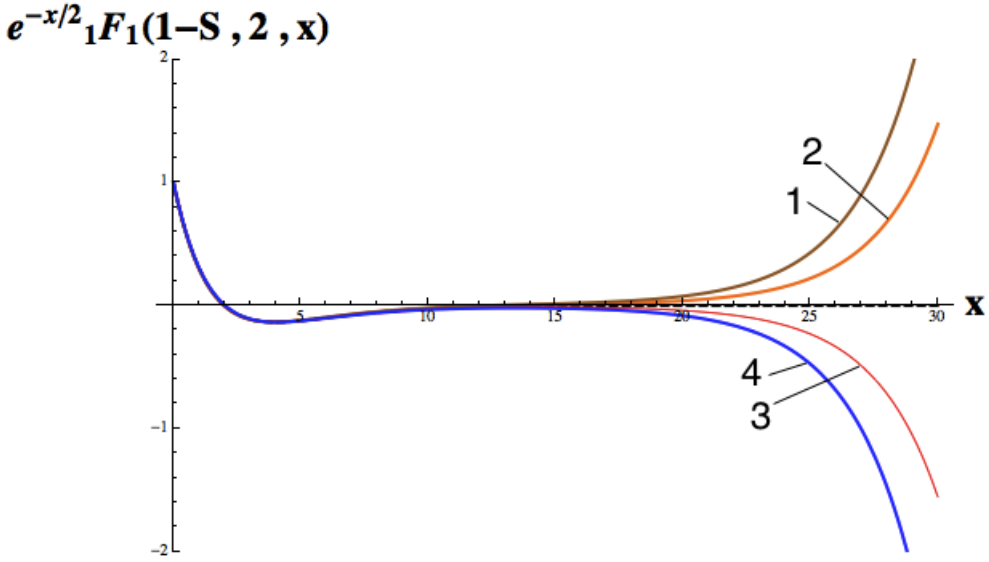

Figure 4.2: The $e^{-x/2}{}_1\mathbf{F_1}(1-S,2,x)$ function vs x, for some values of S around 2. From the figure, the black dashed curve has $S = 2$ (for large values of x, it is essentially coincident with the x-axis), the orange curve (2) has $S = 2.01$, the red curve (3) has $S = 1.99$, the brown curve (1) has $S = 2.02$, and the blue curve (4) has $S = 1.98$. We find that all S values diverge at $x \to \infty$ except for $S = 2$.

It is clear from Figures 4.2 and 4.3 that both terms in Eq.(4.19) satisfy the two boundary conditions which are $\psi(0) = const.$, and $\psi(\infty) = 0$, if and only if S equals integers $n = 1, 2, 3, \cdots$. It can also be proved from the definition of both ${}_1\mathbf{F_1}$ and $\mathbf{U}$ functions Eq.(4.15). Therefore, from this condition we can find the eigenvalues E_n as

$$\begin{aligned} n &= S; \\ n^2 &= -\tfrac{UA^2}{4E}; \\ E_n &= -\tfrac{UA^2}{4n^2}. \end{aligned} \tag{4.20}$$

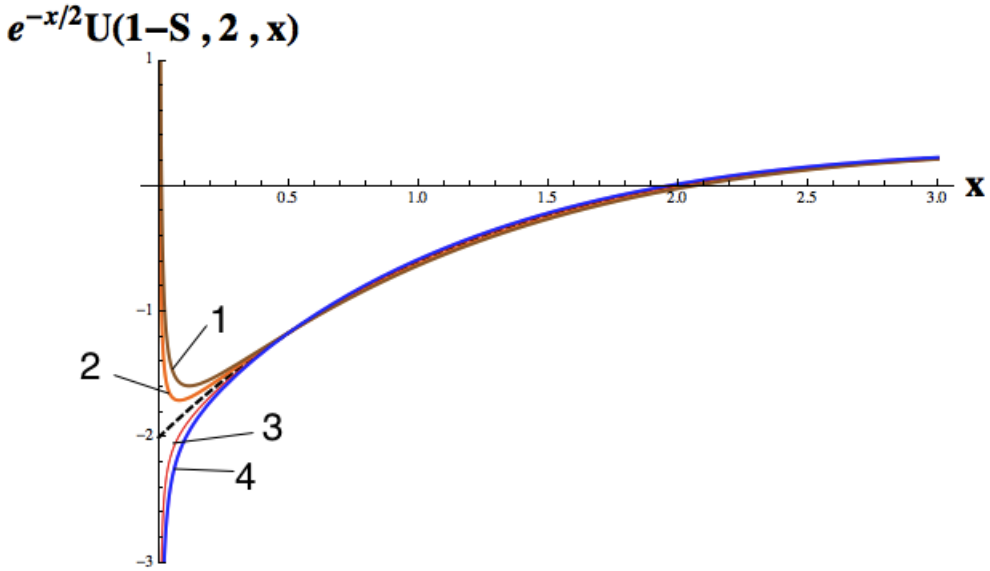

Figure 4.3: The $e^{-x/2}\mathbf{U}(1-S,2,x)$ function vs x, for some values of S around 2. From the figure, the black dashed curve has $S=2$, the orange curve (2) has $S=2.01$, the red curve (3) has $S=1.99$, the brown curve (1) has $S=2.02$, and the blue curve (4) has $S=1.98$. We find that all of S values diverge at $x\to 0$ except for $S=2$. Also, all of these curves go to zero at $x\to\infty$.

These are the well-known Coulomb eigenvalues with n from 1 to ∞. Then, let us talk about the radial wave function. According to Schrödinger [39], Messiah [40] and others [41] [38], the exact radial wave function of the Coulomb potential is the term which has ${}_1\mathbf{F_1}$ function, or

$$\psi_1 = B\delta e^{-\frac{\delta}{2}r}\,{}_1\mathbf{F_1}(1-S,2,\delta r). \tag{4.21}$$

Also, because of Figure 4.3 we can say that the **U** function is also a possible solution since it satisfies both boundary conditions if S is a positive integer. We can see if S is not an integer number, the **U** function will diverge at the origin. Therefore, we also can write the radial wave function as

$$\psi_2 = C\delta e^{-\frac{\delta}{2}r}\,\mathbf{U}(1-S,2,\delta r) \tag{4.22}$$

Eqs.(4.21, 4.22) are equivalent if and only if $S=1,2,3,\cdots$. We also can emphasize this fact by using the Laguerre polynomial representation [33]. **U** and ${}_1\mathbf{F_1}$ functions have the following representation

when $a = 1 - n$ in Eq.(4.15) with n equal to $1, 2, 3, 4, \cdots$.

$$\begin{aligned} {}_{\mathbf{1}}\mathbf{F}_{\mathbf{1}}(1-n, 2, x) &= \tfrac{(n-1)!}{(2)^{(n-1)}} L^1_{n-1}(x); \\ \mathbf{U}(1-n, 2, x) &= (-1)^{n-1}(n-1)! L^1_{n-1}(x), \end{aligned} \tag{4.23}$$

where $L^1_n(x)$ is the associated Laguerre polynomial

$$L^{\alpha}_n(x) = \frac{x^{-\alpha}e^x}{n!}\frac{d^n}{dx^n}\left(e^{-x}x^{n+\alpha}\right) = x^{-\alpha}\frac{\left(\frac{d}{dx}-1\right)^n}{n!}x^{n+\alpha}. \tag{4.24}$$

However, from Eq.(4.23) we have

$$\mathbf{U}(1-n, 2, x) = (-1)^{n-1}(2)^{(n-1)}\,{}_{\mathbf{1}}\mathbf{F}_{\mathbf{1}}(1-n, 2, x), \tag{4.25}$$

which means that they are proportional and the only difference between them is the coefficient in front of ${}_{\mathbf{1}}\mathbf{F}_{\mathbf{1}}$. Accordingly, both equations Eq.(4.21) and Eq.(4.22) are equivalent to the radial wave functions in the Coulomb potential, and we are free to pick any one of them. It is to be noted that, if we insert l in solving this DE, it will not affect the fact that the two confluent hypergeometric functions are equivalent if a in Eq.(4.15) is a negative integer.

The final step is that of substituting the value of E_n inside δ, we find

$$\delta = \frac{UA}{n}, \qquad \frac{\delta}{2} = \frac{1}{a_0 n}, \qquad a_0 = \frac{2}{UA}, \qquad S = n, \tag{4.26}$$

where a_0 is the Bohr radius. Then, the radial wave function is rewritten as

$$\psi(r) = \frac{CUA}{n}e^{-\frac{r}{a_0 n}}(-1)^{n-1}(n-1)!L^1_{n-1}(\frac{2r}{a_0 n}), \tag{4.27}$$

where C is a normalization constant.

4.3 Cutoff Coulomb potential

The cutoff Coulomb potential is obtained by just adding a cutoff which is the finite spherical potential to the Coulomb potential. We wish to know whether this potential will behave like the Coulomb potential, i.e. does it have an infinite or a finite NBSE? Let us start by defining this potential as

follows:

$$V_{ccou}(r) = \begin{cases} -\frac{A}{R_0} & \text{if } 0 < r < R_0; \\ -\frac{A}{r} & \text{if } r > R_0, \end{cases} \tag{4.28}$$

which is shown in Figure 4.4.

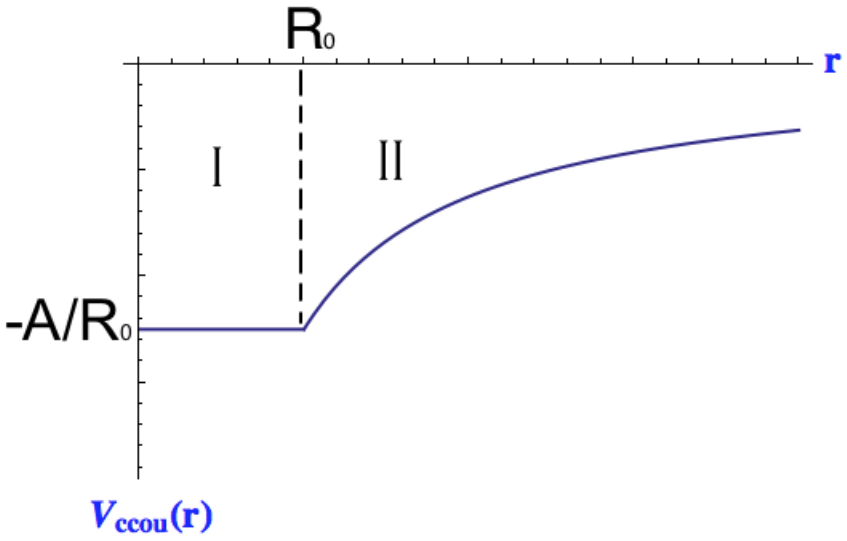

Figure 4.4: The cutoff Coulomb potential, with a cutoff strength A/R_0. R_0 is the cutoff radius.

Then, before we proceed with solving for this potential we wish to give a summary about what may be expected. All the estimating methods in Ch.1 suggest that the NBSE of this potential is infinite, which means this potential is most likely to have an infinite NBSE, and this is what we will find. The NBSE from the spherical potential Eq.(4.1) with $V_0 \equiv A/R_0$, and $R_0 \equiv R_0$ is

$$N = \frac{1}{\pi}\sqrt{AUR_0} + \frac{1}{2}. \tag{4.29}$$

When $R_0 \to \infty$, we expect to observe an infinite number of bound states, even though the strength is decreasing when $R_0 \to \infty$.

We start by solving SE, for region **I**

$$\frac{1}{U}\frac{d^2\chi_1}{dr^2} + \left[E + \frac{A}{R_0}\right]\chi_1 = 0, \tag{4.30}$$

The solution is taken from Eq.(4.3) (see Eq.(3.28))

$$\frac{\psi_1'(r)}{\psi_1(r)} = q\cot(qr) - \frac{1}{r}, \qquad \text{with} \qquad q = \sqrt{U\left(E + \frac{A}{R_0}\right)}. \tag{4.31}$$

Then, the second region **II** has the following DE:

$$-\frac{1}{U}\frac{\partial^2\chi_2}{\partial r^2} - \frac{A}{r}\chi_2 = E\chi_2. \tag{4.32}$$

the solution of this DE is taken from Eq.(4.19)

$$\psi_2(r) = e^{-\frac{\delta}{2}r}\delta\Big[B\,{}_1\mathbf{F}_1(1-S,2,\delta r) + C\,\mathbf{U}(1-S,2,\delta r)\Big]; \qquad S = \frac{UA}{\sqrt{-4UE}}; \qquad \delta = \sqrt{-4UE}. \tag{4.33}$$

According to the two Figures 4.2, 4.3 and the discussion in the previous section, we will keep the **U** function and set the coefficient B to zero since the ${}_1\mathbf{F}_1$ function does not satisfy the boundary condition at ∞. Here we cannot take S to be an integer since we will connect this expression with the spherical potential expression at R_0. Therefore, S can take on any value, and then the **U** function is the only possible solution. The divergence at the origin in Figure 4.3 does not matter since the **U** function is taken only to $r = R_0$. Then,

$$\psi_2(r) = C\delta e^{-\frac{\delta}{2}r}\mathbf{U}(1-S,2,\delta r). \tag{4.34}$$

Now, let us find the first derivative of this equation, using

$$\frac{d\mathbf{U}(a,b,x)}{dx} = -a\mathbf{U}(a+1,b+1,x). \tag{4.35}$$

Therefore, ψ_2' is given as

$$\psi_2' = -\frac{C\delta^2}{2}e^{\frac{-\delta r}{2}}\Big[\mathbf{U}(1-S,2,\delta r) + 2(1-S)\,\mathbf{U}(2-S,3,\delta r)\Big]. \tag{4.36}$$

Then, we find

$$\frac{\psi_2'}{\psi_2} = -\frac{\delta}{2}\left[1 + 2(1-S)\frac{\mathbf{U}(2-S,3,\delta r)}{\mathbf{U}(1-S,2,\delta r)}\right]. \tag{4.37}$$

Let us apply the continuity conditions at $r = R_0$, to find

$$q\cot(qR_0) - \frac{1}{R_0} = -\frac{\delta}{2}\left[1 + 2(1-S)\frac{\mathbf{U}(2-S,3,\delta R_0)}{\mathbf{U}(1-S,2,\delta R_0)}\right], \tag{4.38}$$

by defining $qR_0 \equiv \Omega$ and $\delta R_0 \equiv h$, the condition becomes

$$\Omega\cot(\Omega) - 1 = -\frac{h}{2}\left[1 + 2(1-S)\frac{\mathbf{U}(2-S,3,h)}{\mathbf{U}(1-S,2,h)}\right], \tag{4.39}$$

where

$$\begin{aligned} U &= \tfrac{2m}{\hbar^2}, \\ \Omega &= \sqrt{UR_0^2\left(\tfrac{A}{R_0} + E\right)}, \\ h &= 2\sqrt{-UR_0^2 E}, \\ S &= \tfrac{1}{2}\sqrt{\tfrac{-UA^2}{E}}. \end{aligned} \tag{4.40}$$

Then the energy equation of the cutoff Coulomb potential is given by Eq.(4.39). Indeed, S can take on any positive value. However, let us renormalize the energies E to the Coulomb energies in the previous section. Also, normalize the length R_0 to the Bohr radius, we will find

$$\begin{aligned} E &= \epsilon E_0; \qquad E_0 = \tfrac{UA^2}{4}; \\ R_0 &= \beta a_0; \qquad a_0 = \tfrac{2}{UA}; \\ \Omega &= \sqrt{2\beta\left(1 + \tfrac{\beta\epsilon}{2}\right)}; \qquad \bar{\Omega} = \sqrt{-2\beta\left(1 + \tfrac{\beta\epsilon}{2}\right)}; \\ h &= 2\beta\sqrt{-\epsilon}; \\ S &= \tfrac{1}{\sqrt{-\epsilon}}. \end{aligned} \tag{4.41}$$

Then, when we plot the LHS and the RHS of Eq.(4.39) on the same graph with respect to ϵ^{-1} and a given value of β, we obtain Figure 4.5, and, we find that there exist an infinite NBSE. Also, from this figure we find the LHS gives almost a line close to zero because the value of Ω with small β, gives very small values for all its real domain. In case when $\beta \to 0$ the values of ϵ_n will be

$$\epsilon_n = -\frac{1}{n^2}, \tag{4.42}$$

which are exactly the same eigenvalues as these obtained with the Coulomb potential . Then, by increasing the value β the Ω expression will be an imaginary value, just when the following inequality

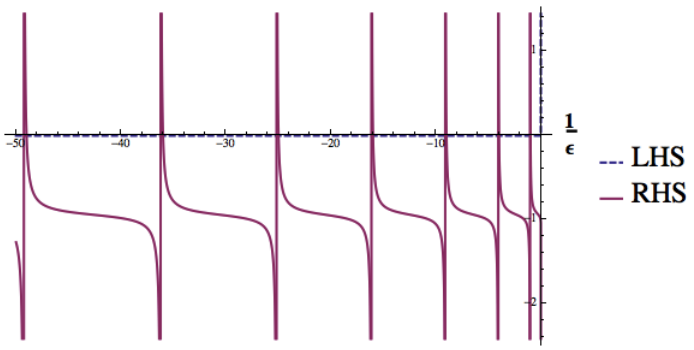

Figure 4.5: The LHS (blue dashed curve) and the RHS (red curve) of Eq.(4.39) with $\beta = 0.01$. The LHS is almost a line equal to 0, and the RHS has an infinite number of intersections with LHS curve as the value $(-1/\epsilon)$ goes to infinity, which means an infinite NBSE.

is satisfied:

$$\epsilon \leq -\frac{2}{\beta}. \tag{4.43}$$

If this inequality is satisfied, we can write $\Omega = i\bar{\Omega}$. The cot function is defined as

$$\cot(x) = i\frac{e^{ix} + e^{-ix}}{e^{ix} - e^{-ix}}. \tag{4.44}$$

Substituting the imaginary value of Ω leads to

$$\cot(i\bar{\Omega}) = i\frac{e^{-\bar{\Omega}} + e^{\bar{\Omega}}}{e^{-\bar{\Omega}} - e^{\bar{\Omega}}} = -i\coth(\bar{\Omega}), \tag{4.45}$$

then, the LHS of Eq.(4.39) becomes

$$\bar{\Omega}\coth(\bar{\Omega}) - 1 \tag{4.46}$$

This prevents the periodicity of the cot function.

Now, let us study the final expression for the energy Eq.(4.39). This expression yields an infinite number of bound state energies. Let us plot the values of ϵn^2 vs n, where n is the principal quantum number for various values of β. When $\beta \to 0$, we should get a line equal to -1. This is what we is found in Figures 4.6 and 4.7.

When $\beta >> 1$, we expect the first few energies to have almost the same values of the finite spherical potential. However, when β is large enough we use the approximate energy expression of

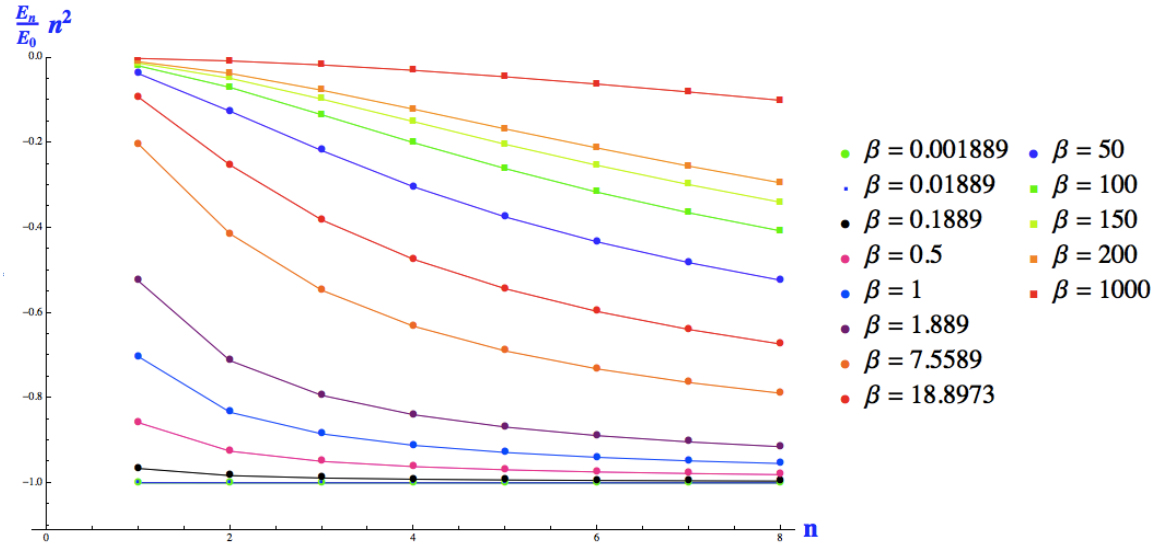

Figure 4.6: Some energies of the cutoff Coulomb potential for various value of β. When $\beta \to 0$ ($\beta = 0.001889$) we get a line equal to -1 which are exactly the same eigenvalues as for the Coulomb potential. For an extreme cutoff $\beta >> 1$, the first few energies will have almost the same values as those of the spherical well potential. Curves close to -1 correspond to smallest values of β.

the spherical potential Eq.(4.2)

$$\begin{aligned} E_n &= \frac{n^2\pi^2}{UR_0^2} - \frac{A}{R_0}; \\ E_n &= \frac{n^2\pi^2 UA^2}{4\beta} - \frac{UA^2}{2\beta}; \\ \epsilon &= \frac{E_n}{E_0} = \frac{n^2\pi^2}{\beta^2} - \frac{2}{\beta}; \\ \frac{E_n}{E_0}n^2 &= \left[\frac{n^2\pi^2}{\beta^2} - \frac{2}{\beta}\right] n^2. \end{aligned} \tag{4.47}$$

The final expression estimates the value of the first few energies to high precision when $\beta >> 1$.

4.4 Cutoff inverse square potential

The cutoff inverse square potential allows a connection of the finite spherical potential near the origin to the inverse square potential at $r \to \infty$. The inverse square potential alone has an infinite or zero number of bound states as shown in [42]. Also, all estimating methods in Ch.1 indicate there is an infinite NBSE for this potential, and we will observe the same results with our computations.

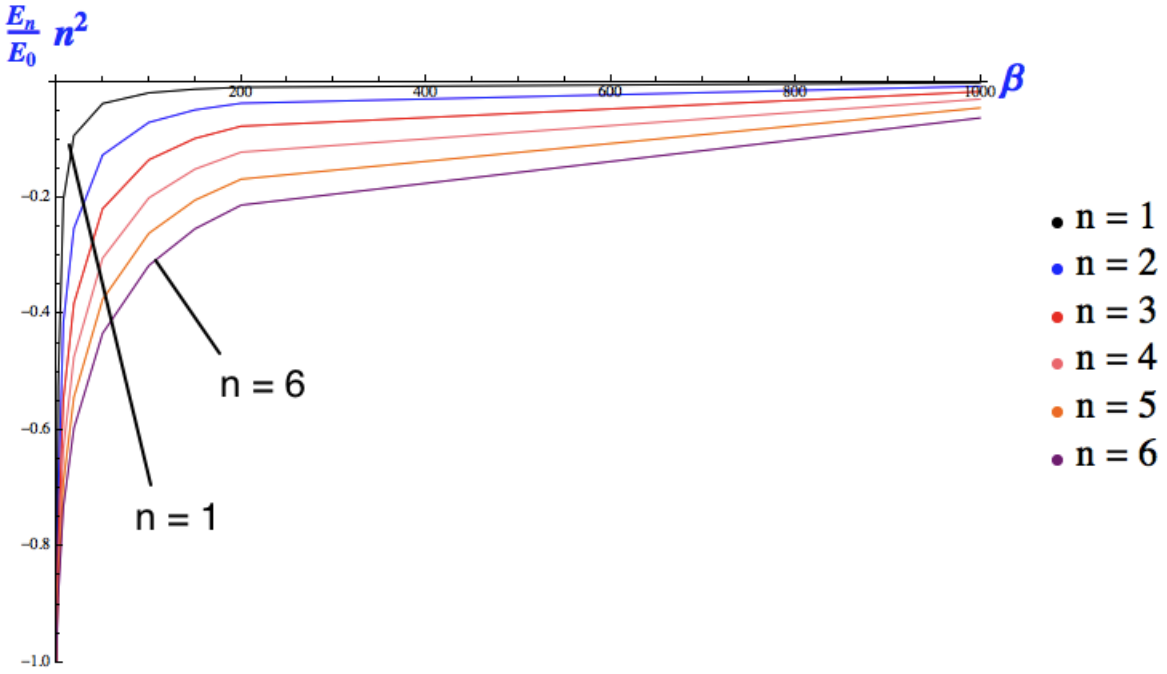

Figure 4.7: Some energies of the cutoff Coulomb potential for various values of n. As we can see all curves start from -1 which are the Coulomb energies, and end with the extreme spherical potential Eq.(4.47).

Let us start with the definition of this potential

$$V(r) = \begin{cases} -\frac{A}{R_0^2} & \text{if } 0 < r < R_0; \\ -\frac{A}{r^2} & \text{if } r > R_0. \end{cases} \tag{4.48}$$

Now we calculate the NBSE just for the spherical potential from Eq.(4.1), where V_0 is A/R_0^2, and R_0 is the same as in Fig 4.8. We find

$$N = \frac{\sqrt{UA}}{\pi} + \frac{1}{2}. \tag{4.49}$$

This result is independent of R_0, which means the spherical potential is insensitive to the value of R_0 if the strength varies as A/R_0^2. Therefore, we expect to see this independence of $R_0 > 0$ in the

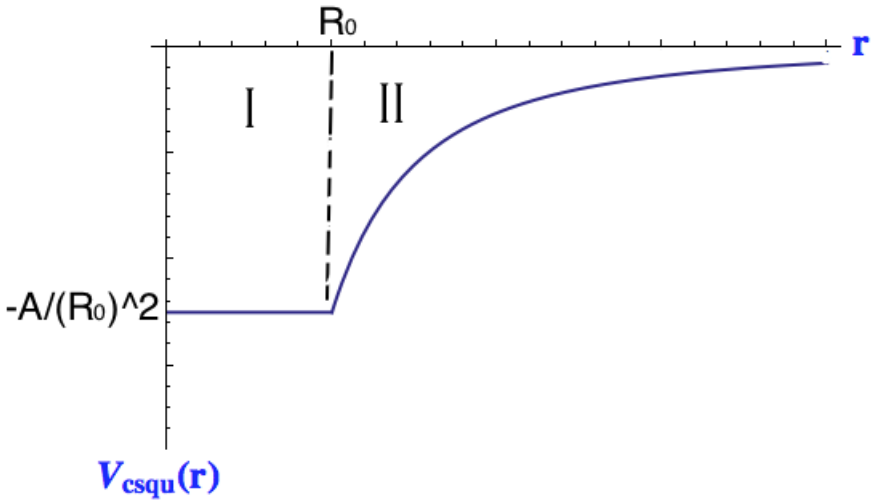

Figure 4.8: The cutoff inverse square potential, with a cutoff strength A/R_0^2. **I** is the first region, and **II** is the second region. R_0 is the cutoff radius.

solution. Then, the SE for the first region **I** is

$$-\frac{1}{U}\frac{\partial^2\chi_1}{\partial r^2} - \frac{A}{R_0^2}\chi_1 = E\chi_1. \tag{4.50}$$

The solution of this expression is (see Eq.(4.3))

$$\frac{\psi_1'(r)}{\psi_1(r)} = q\cot(qr) - \frac{1}{r}, \qquad \text{with} \qquad q = \sqrt{U\left(E + \frac{A}{R_0^2}\right)}. \tag{4.51}$$

Then, let us consider the second region **II**. The radial SE wave equation is

$$-\frac{1}{U}\frac{\partial^2\chi_2}{\partial r^2} - \frac{A}{r^2}\chi_2 = E\chi_2, \tag{4.52}$$

or

$$\frac{\partial^2\chi_2}{\partial r^2} + \frac{UA}{r^2}\chi_2 + UE\chi_2 = 0. \tag{4.53}$$

Now, let us define the following

$$\alpha^2 = UA; \qquad\qquad \delta^2 = UE. \tag{4.54}$$

Then, Eq.(4.53) becomes

$$\frac{\partial^2 \chi_2}{\partial r^2} + \frac{\alpha^2}{r^2}\chi_2 + \delta^2 \chi_2 = 0. \tag{4.55}$$

Changing variables,

$$\chi_2 = \sqrt{r} y, \tag{4.56}$$

we get

$$\sqrt{r}\frac{d^2 y}{dr^2} + \frac{1}{\sqrt{r}}\frac{dy}{dr} + y\left(\delta^2\sqrt{r} + \frac{\alpha^2\sqrt{r}}{r^2} - \frac{1}{4r^{3/2}}\right) = 0. \tag{4.57}$$

Let us multiply this equation by $r^{3/2}$. Then we get

$$r^2\frac{d^2 y}{dr^2} + r\frac{dy}{dr} + y\left(\delta^2 r^2 + \alpha^2 - \frac{1}{4}\right) = 0. \tag{4.58}$$

Changing the variable r to x as

$$x = \delta r, \tag{4.59}$$

Eq.(4.58) becomes

$$x^2\frac{d^2 y}{dx^2} + x\frac{dy}{dx} + \left[x^2 - \left(\frac{1}{4} - \alpha^2\right)\right] y = 0. \tag{4.60}$$

This equation has the following form

$$z^2\frac{d^2 Q}{dz^2} + z\frac{dQ}{dz} + \left[z^2 - \gamma^2\right] Q = 0 \tag{4.61}$$

This DE is so-called Bessel's differential equation, and its general solution is:

$$Q = BJ_\gamma(z) + DY_\gamma(z) = BJ[\gamma, z] + DY[\gamma, z], \tag{4.62}$$

where B, D are constants to be determined, and Y, J are Bessel functions, and they are defined as

$$\begin{array}{rcl} J_\alpha(x) & = & J[\alpha, x] = \sum_{m=0}^{\infty} \frac{(-1)^m}{m!\Gamma(m+\alpha+1)} \left(\frac{x}{2}\right)^{2m+\alpha}; \\ Y_\alpha(x) & = & Y[\alpha, x] = \frac{J_\alpha(x)\cos(\alpha\pi) - J_{-\alpha}(x)}{\sin(\alpha\pi)}. \end{array} \tag{4.63}$$

Then, by comparing Eq.(4.61) with equation (4.60), we find that $\gamma = \frac{1}{4} - \alpha^2$, and the solution is given as

$$y = BJ[\sqrt{\frac{1}{4} - \alpha^2}, x] + DY[\sqrt{\frac{1}{4} - \alpha^2}, x]. \tag{4.64}$$

Now, if we define the following:

$$B = G + F, \qquad D = i(G - F). \tag{4.65}$$

We get

$$y = G\,H^{(1)}[\sqrt{\frac{1}{4} - \alpha^2}, x] + F\,H^{(2)}[\sqrt{\frac{1}{4} - \alpha^2}, x]. \tag{4.66}$$

where $H^{(1)}$ and $H^{(2)}$ are the Hankel functions, and their definitions are

$$H_\gamma^{(1)}[x] = H^{(1)}[\gamma, x] = J_\gamma[x] + iY_\gamma[x]; \qquad H_\gamma^{(2)}[x] = H^{(2)}[\gamma, x] = J_\gamma[x] - iY_\gamma[x]. \tag{4.67}$$

Then, the full solution in the second region ψ_2 is

$$\psi_2(r) = \frac{1}{\sqrt{r}} \left(G\,H^{(1)}[\sqrt{\frac{1}{4} - \alpha^2}, \delta r] + F\,H^{(2)}[\sqrt{\frac{1}{4} - \alpha^2}, \delta r] \right). \tag{4.68}$$

The value of δ is always an imaginary number, and $\sqrt{\frac{1}{4} - \alpha^2}$ can be either imaginary or real. That is why we have used the Hankel functions. Now which of the Hankel functions satisfies the boundary conditions with $r \to \infty$. Therefore, we have plotted both terms of Eq.(4.68) for some values of δ and α. From Figures 4.9 and 4.10, we conclude that the only possible function to represent the physical solution of this potential is the $H^{(1)}$ function. Therefore, we put $F = 0$. Then, Eq.(4.68) becomes

$$\psi_2 = G\frac{H^{(1)}[\theta, \delta r]}{\sqrt{r}}, \tag{4.69}$$

where

$$\sqrt{\theta} = \sqrt{\frac{1}{4} - \alpha^2}. \tag{4.70}$$

From Ref. [33], one finds that the derivative of the $H^{(1)}$ function is

$$\frac{dH^{(1)}[\gamma, z]}{dz} = \frac{H^{(1)}[\gamma - 1, z] - H^{(1)}[\gamma + 1, z]}{2}. \tag{4.71}$$

Then, the derivative of Eq.(4.69) is

$$\frac{d\psi_2}{dr} = \frac{G}{2\sqrt{r}} \left[-\frac{H^{(1)}[\theta, \delta r]}{r} + \delta[H^{(1)}[\theta - 1, \delta r] - H^{(1)}[\theta + 1, \delta r]] \right]. \tag{4.72}$$

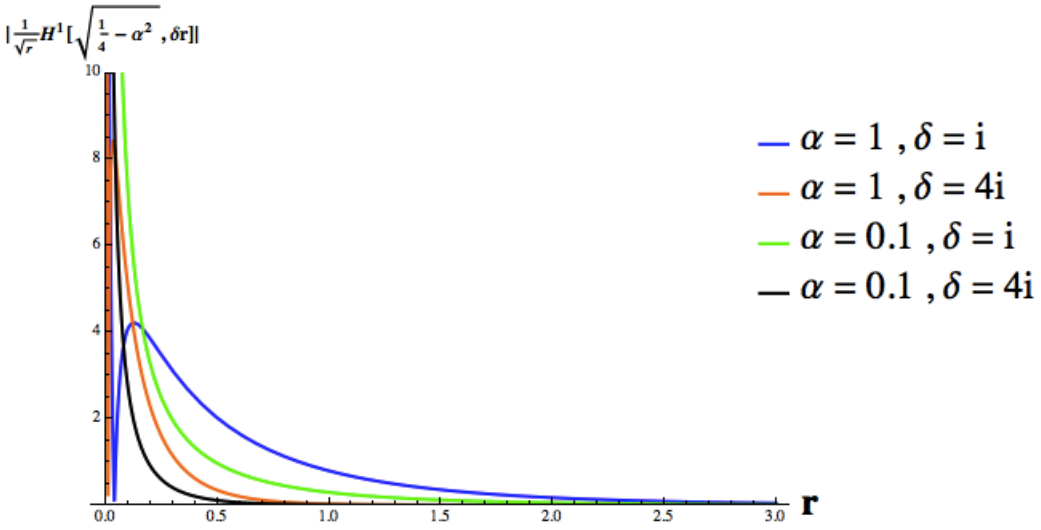

Figure 4.9: Plot of $\frac{1}{\sqrt{r}}H^1[\sqrt{0.25-\alpha^2},\delta r]$ vs r for some values of both δ and α. There is a singularity at the origin.

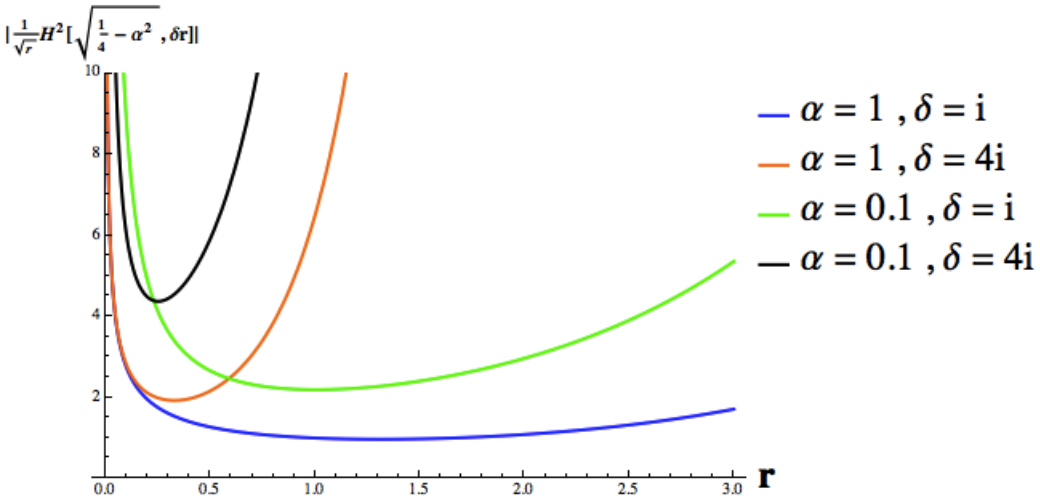

Figure 4.10: Plot of $\frac{1}{\sqrt{r}}H^2[\sqrt{0.25-\alpha^2},\delta r]$ vs r for some values of both δ and α. There are singularities at both the origin and as $r \to \infty$.

Then, we find

$$\frac{\psi_2'}{\psi_2} = -\frac{1}{2r} + \frac{\delta}{2}\frac{H^{(1)}[\theta-1,\delta r] - H^{(1)}[\theta+1,\delta r]}{H^{(1)}[\theta,\delta r]}. \tag{4.73}$$

Let us connect both solutions Eq.(4.60) and Eq.(4.73) at $r = R_0$; we find

$$\Omega \cot \Omega - \frac{1}{2} = \frac{h}{2} \frac{H^{(1)}[\theta - 1, h] - H^{(1)}[\theta + 1, h]}{H^{(1)}[\theta, h]}, \tag{4.74}$$

where

$$\begin{aligned} U &= \tfrac{2m}{\hbar^2}, \\ \Omega &= \sqrt{U R_0^2 \left(\tfrac{A}{R_0^2} + E\right)}, \\ h &= \sqrt{U R_0^2 E}, \\ \theta &= \sqrt{\tfrac{1}{4} - UA}. \end{aligned} \tag{4.75}$$

Then the energy equation of the cutoff inverse square potential is given by Eq.(4.74). From this expression we find that the NBSE is infinite when UA is larger than 0.25, which means when θ is a pure imaginary value (see Figure 4.11). On the other hand, when θ is a real number there will be no bound states. Therefore, the outcome of this potential is one of two possibilities either infinite NBSE or zero depending on the value of AU. Also, when we plot Eq.(4.74) and decreased the value of $R_0 \to 0$, the first bound state energy always becomes close to A/R_0^2. Accordingly, it is better to normalize the energy to $E_0 = \frac{A^2 U}{R_0^2}$. Since the energies take on values on the logarithmic scale (see

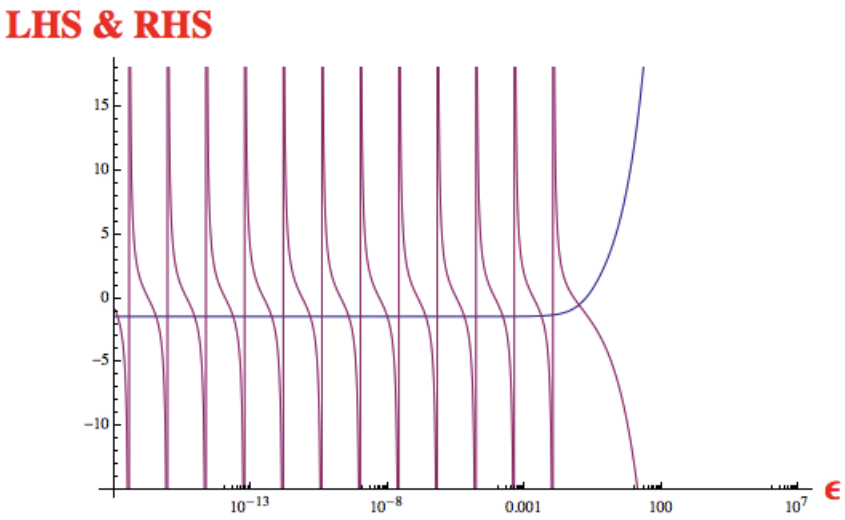

Figure 4.11: The LHS and RHS of the energy equation of the cutoff inverse square potential Eq.(4.74) for $\rho = UA = 4$. As $\epsilon \to 0$, Fig. 4.11 shows zeros occurring with a constant period, hence the plot is on a logarithmic scale in ϵ this implies an infinite NBSE.

Figure 4.11), we define the following

$$\begin{aligned} \epsilon &= \frac{E}{E_0}, \qquad E_0 = \frac{A^2 U}{R_0^2}, \\ \rho &= UA, \\ \Omega &= \sqrt{\rho(\rho\epsilon + 1)}, \\ h &= \rho\sqrt{\epsilon}, \\ \theta &= \sqrt{\tfrac{1}{4} - \rho}, \end{aligned} \tag{4.76}$$

where ρ and ϵ are dimensionless quantities. We notice in this representation, R_0 is hidden in ϵ, so we know the curve of the $E/E_0 = \epsilon$ vs n. Also, based on the properties we found from Eq.(4.74), we find them analytically by analyzing the function $H^{(1)}$. We proceed graphically. Then, from Figure

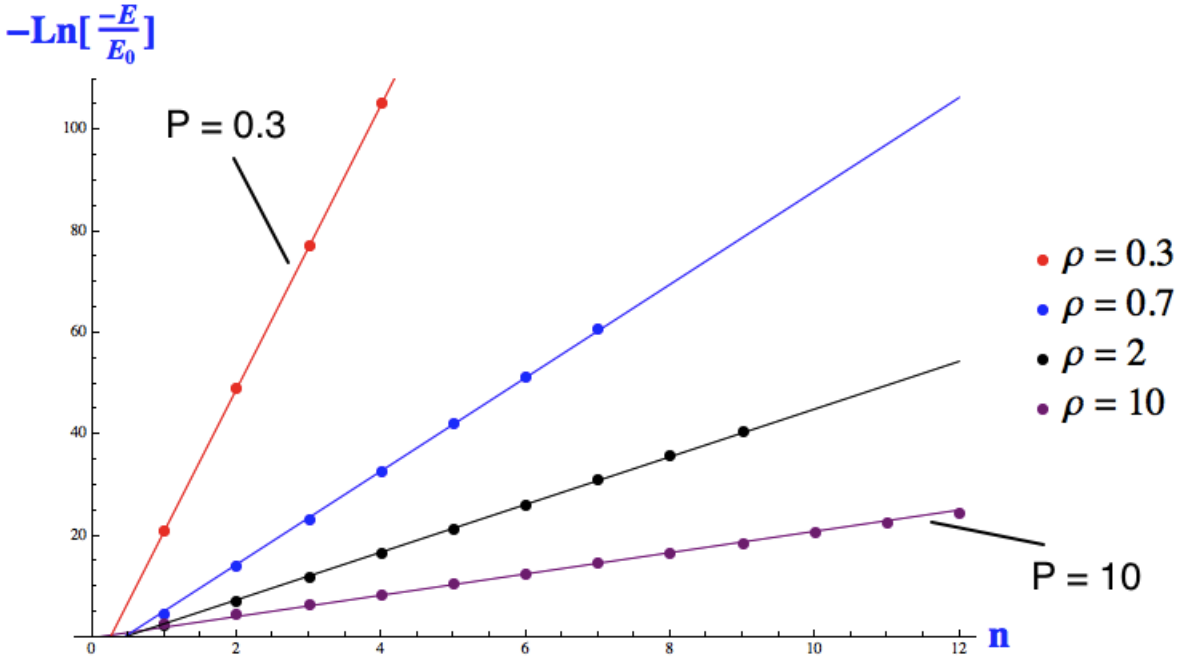

Figure 4.12: Some of the eigenvalues of the cutoff inverse square potential for some values of ρ. The linear behaviour of $-\ln(-\epsilon_n)$ with n is clear.

4.12 we find how the eigenvalues vary with n. Since the curves appear as lines, we can write the following expression only if ρ is greater than 0.25.

$$-\ln\left(\frac{E_n}{E_0}\right) = a(\rho)n - b(\rho) \tag{4.77}$$

where $a(\rho)$ and $b(\rho)$ are expressions that need to be determined. Then, we rewrite it as

$$E_n = -\frac{\rho A}{R_0^2}\exp\Big(b(\rho) - a(\rho)n\Big); \qquad n = 1, 2, 3, \cdots; \qquad \rho > 0.25. \tag{4.78}$$

To conclude, the cutoff inverse square potential is not very different from the inverse square potential in terms of NBSE and the general behaviour of E_n. Morse and Feshbach [42] in their book showed that the inverse square potential has eigenvalues proportional to $\exp(Cn)$, where C is a constant that depends on ρ. Furthermore, this potential is really dependent on the value of ρ more than the value of R_0.

4.5 Cutoff inverse cubic potential

The cutoff inverse cubic potential is a combination of the spherical potential and the inverse cubic potential. This potential cannot be solved analytically; therefore, the numerical method explained in Ch.2 needs to be used. All the estimating methods in Ch.1 predict that this potential has a finite NBSE. The definition of this potential is

$$V(r) = \begin{cases} -\frac{A}{R_0^3} & \text{if } 0 < r < R_0; \\ -\frac{A}{r^3} & \text{if } r > R_0, \end{cases} \tag{4.79}$$

and it is drawn in Figure 4.13. First, we will give some examples of what the estimating methods tell us. We show two of these methods, which are: the Calogero and Cohn upper limit Eq.(1.24), and the Bargmann-Schwinger bound Eq.(1.19).

$$N \approx \frac{6}{\pi}\sqrt{\frac{AU}{R_0}}; \qquad \text{the Calogero and Cohn upper limit.} \tag{4.80}$$

$$N < \frac{3AU}{2R_0}; \qquad \text{the Bargmann-Schwinger bound.} \tag{4.81}$$

As we find from these limits, they suggest the value AU/R_0 to be the fixed number expression (FNE) of this potential. Therefore, we assume this to be the FNE, and we find that this choice is correct:

$$\mathbf{G_{ccub}} = \frac{AU}{R_0}. \tag{4.82}$$

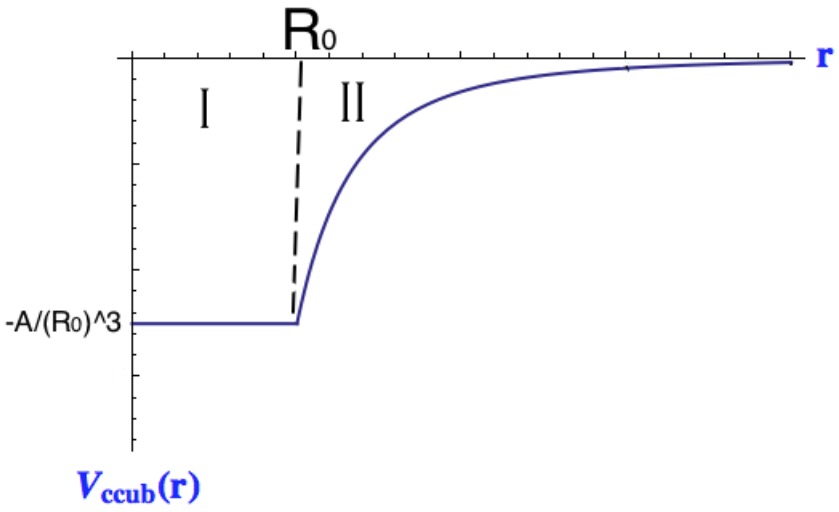

Figure 4.13: The cutoff inverse cubic potential, with a cutoff strength A/R_0^3. **I** is the first region $0 < r < R_0$, and **II** is the second region $R_0 < r < \infty$. R_0 is the cutoff radius.

However, we find the FNE directly just from rescaling the SE as explained in Sec. 3.2. Then, the NBSE is calculated just from the spherical potential since we know its exact expression Eq.(4.1), with $V_0 \equiv A/R_0^3$, and $R_0 \equiv R_0$. We find

$$N = \frac{1}{\pi}\sqrt{\frac{AU}{R_0}} + \frac{1}{2}. \tag{4.83}$$

This is the same FNE as in Eq.(4.82). If $R_0 \to 0$, Eq.(4.83) tells us that we will have an infinite NBSE arising just from the spherical potential. Therefore, we expect that when R_0 is very small, the NBSE will be a large number. However, this fact is true also for the inverse cubic potential since it has an infinite NBSE, where there is no cutoff at the origin. (this results also follows from any one of the estimating methods discussed in Chapter 1. [11].)

Next, let us prepare to find the matrix elements of $\mathbf{H_{nm}}$ in Eq.(2.11) for the case $l = 0$. The first region **I** in Figure 4.13 has just the spherical potential, and we have already found the matrix elements of this potential in Eq.(2.16). We just have to replace V_0 by its value A/R_0^3. The second region **II** of this potential has a matrix element similar to the Coulomb potential in Eq.(2.20), with

a difference in the power of r. Then, the matrix elements are

$$\mathbf{H_{nm}} = \delta_{nm} E_n^0 - \frac{A}{\pi R_0^3}[g(n-m) - g(n+m)] + \frac{A}{b}[s(n-m) - s(n+m)], \tag{4.84}$$

where

$$E_n^0 = \frac{\pi^2 n^2}{U b^2}; \tag{4.85}$$

$$g(n) = \frac{sin(n\pi R_0/b)}{n}, \tag{4.86}$$

and

$$s(n) = \int_{R_0}^{b} \frac{1 - cos(n\pi r/b)}{r^3}\, dr. \tag{4.87}$$

Here b is the size of the infinite well, and U is $\frac{2m}{\hbar^2}$.

Now, normalize the energy by the value $E_0 = \frac{A}{R_0^3}$, so the energy will be represented as $\epsilon_n = \frac{E_n}{E_0}$. Then, the FNE Eq.(4.82) is investigated

R_0	U	A	$\mathbf{G_{ccub}} = \frac{AU}{R_0}$	ϵ_1	ϵ_2	$b\,[R_0]$	n_{max}	N
0.5	1	1	2	−0.0912655	− − −	50	1000	1
4	2	4	2	−0.0912655	− − −	50	1000	1
20	40	1	2	−0.0912655	− − −	50	1000	1
0.01	0.2	0.1	2	−0.0912655	− − −	50	1000	1
1	1	8	8	−0.538905	−0.00664784	50	1000	2
2	2	8	8	−0.538905	−0.00664784	50	1000	2
4	160	0.2	8	−0.538905	−0.00664784	50	1000	2
0.1	0.01	80	8	−0.538905	−0.00664784	50	1000	2

Table 4.1: Test of the FNE for the cutoff inverse cubic potential $\mathbf{G_{ccub}}$ by the numerical matrix method. b is the range of the infinite well in units of R_0. It is clear that this FNE is correct since when we fix the value of FNE, and change all its parameters, then we always find fixed NBSE. The test has been done for two values of $\mathbf{G_{ccub}}$, 2 and 8. Also, from the table the values of ϵ are always the same when the value of FNE is fixed.

Table 4.1 shows us that when $\mathbf{G_{ccub}}$ is fixed, the NBSE N will be also fixed, and the values of all the ϵ will remain constant. The fixed value of ϵ_n when FNE is fixed implies that this potential is really like any potential with two parameters which has a finite NBSE (see Sec.3.2). Consequently, this potential has a finite NBSE and has a critical point defined in Ch.1. The Figure 4.14 shows the value of $\mathbf{G^c_{ccub}}$, which is

$$\mathbf{G^c_{ccub}} = 1.026\cdots. \tag{4.88}$$

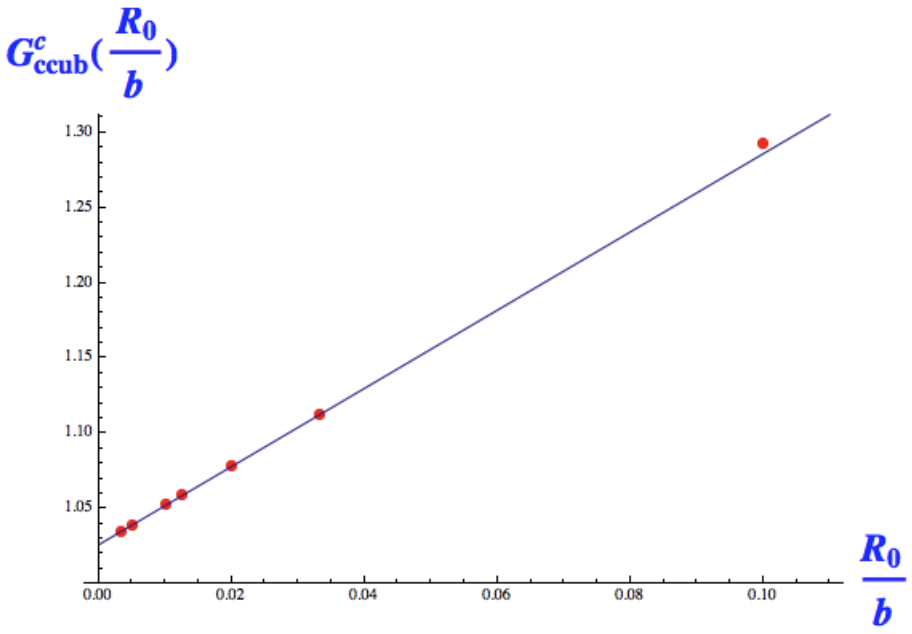

Figure 4.14: Finding the critical point of the cutoff inverse cubic potential by using the matrix method. If $b \to \infty$ the critical point will be $1.026\cdots$.

By using the program for many values of $\mathbf{G_{ccub}}$ we conclude that the NBSE should be proportional to the square root of the FNE of this potential when $\mathbf{G_{ccub}}$ is sufficiently large, which means that

$$N \propto \sqrt{\mathbf{G_{ccub}}}; \qquad \text{when} \qquad \mathbf{G_{ccub}} >> 1. \tag{4.89}$$

This result agrees with what is given in Ref. [17].

Chapter 5

Discussion and concluding remarks

5.1 Discussion

This section provides some general discussion about all the properties for bound state energies which have been calculated. In this section, we point out the most accurate estimating methods for each criterion. However, the only property of bound state energies that will not be discussed is the eigenvalues since they have been considered, and have been obtained with very accurate numerical methods in this thesis. These methods do not just provide the eigenvalues, they also provide the eigenfunctions.

The properties that we will discuss in this chapter are: NBSE, FNE, the critical conditions, and the infinite or finite NBSE.

5.1.1 Number of bound state energies

The number of bound state energies (NBSE) is one of the issues that motivated this thesis. We have reviewed many estimating methods in Ch.1 to determine the upper and lower limits. The most accurate and most recent one is discussed in Ch.3. These are the Brau and Calogero limits. We found that these limits worked very well for our chosen potentials. In particular, for the potentials with two parameters, we observed that these limits are close to the exact NBSE. Moreover, Brau [5] [6] has compared the Brau-Calogero limits with other limits described in Ch.1, and Brau found that the best lower and upper limits are indeed the Brau-Calogero limits, Eqs.(3.17, 3.18). Therefore, if one wishes to estimate the NBSE before solving SE, the Brau-Calogero limits should be used. However,

sometimes there is one difficulty, which is determining p and q in Eq.(3.19). Accordingly, if finding p or q is complicated, one can either neglect them or make an approximation to find p and q in some interval.

From our study of NBSE as it appears in Ch.3 and from the proof of Calogero [17] for the coupling constant g, where in the case $g \to \infty$ it was proved that N_l grows proportionally to g, it may be stated that the NBSE N is usually proportionally to $\sqrt{\mathbf{G}}$ when $\mathbf{G} \to \infty$, where $\mathbf{G}$ is the FNE in its simplest formula, that it has at least one term proportional to U, where U is $2m/\hbar^2$.

5.1.2 Fixed number expression

The fixed number expression (FNE) is one of our suggestions to simplify the representation of NBSE. This expression groups the eigenvalues depending on their NBSE. In other words, if we find this expression for a potential, we can fix it, and vary the potential's parameters without affecting the NBSE. For two-parameter potentials, the FNE is very easy to find, and any one of the estimating methods will be sufficient to give this expression. In addition, the FNE for two-parameter potentials gives an additional feature, which is fixing the normalized eigenvalues as proved in Eq.(3.22). On the other hand, for potentials with three parameters, the full FNE becomes harder to find even if there is an energy equation after solving the SE. However, the FNE is always implicit within the energy equation, and the question is how to extract it from the energy equation.

Any energy equation with a finite NBSE with more than one parameter as Eq.(3.94) for the spherical potentail shell, has at least one function that has an infinite number of zeros. However, let us consider the energy equation when $E \to 0$, and let the function with infinite zeros be $P(x)$, where x is one or a group of parameters. It could be $\mathbf{W_c} = UV_0R_0^2$, which is defined in Ch.(3), so the energy equation is written as

$$P(x) = M(y), \tag{5.1}$$

where M is a function with one zero or more, and y is another group of the potential parameters, or it could be $\mathbf{g} = UV_0a^2$ which is defined in Ch.(3). Then, if $P(x)$ is a periodic function such as cot function, we can write

$$P(x + \lambda) = P(x), \tag{5.2}$$

where λ is the period, and thus

$$\lambda = P^{-1}[M(y)] - x, \tag{5.3}$$

where P^{-1} is the inverse function of the periodic function such as $\cot^{-1}(x)$. In equation (5.3) λ is the FNE. We used this approach for determining the FNE for the finite spherical potential shell Eq.(3.100). Then, if P is not a periodic function such as $Ai(x)$ function, we can write

$$P(x + F(x, \lambda)) = P(x), \tag{5.4}$$

where $F(x, \lambda)$ is the a function which insure the equation (5.4) is satisfied. However, determining $F(x, \lambda)$ is usually hard, so finding the asymptotic behaviour is usually sufficient to get an approximation of F. Then, by using Eq.(5.1), we write

$$x + F(x + \lambda) = P^{-1}[M(y)]. \tag{5.5}$$

This approach is used in the cutoff triangular potential. In general, for three-parameter potentials or more, the FNE is usually implicit, and very hard to determine. Therefore, if we require finding the full range of the FNE, we can do it numerically from Eq.(5.1), where it is the generalized energy equation. For instance, if the second intersection point of Eq.(5.1) corresponds to $N = 2$, then we find the intersection point for each value of y in the second curve. That will give us the critical curve of the second bound state, which means the second bound state will not appear lower than this curve, and above this curve the second bound state will appear. In order to illustrate that, we provide some critical curves for different values of N for the spherical potential shell in Figure 5.1. However, these critical curves for an arbitrary N in **g**-rep usually have a behavior similar to the original critical curve $N = 1$. They have a similar behaviour because they can be obtained from the same equation Eq.(5.1).

The idea of the critical curves for a given N is equivalent to the FNE and easier to obtain for some potentials. However, if any parameter in the potentials with three-parameters is fixed to a given value, then the FNE becomes just like any FNE of two-parameter potentials. For instance, in the Woods-Saxon potential, if we set a to have a specific value, we find the FNE as $UV_0R_0^2$ and there will be no need to have a critical curve.

Last, an approximate FNE from the Brau-Calogero limits Eqs.(3.17, 3.18) can be found, by just considering the first term.

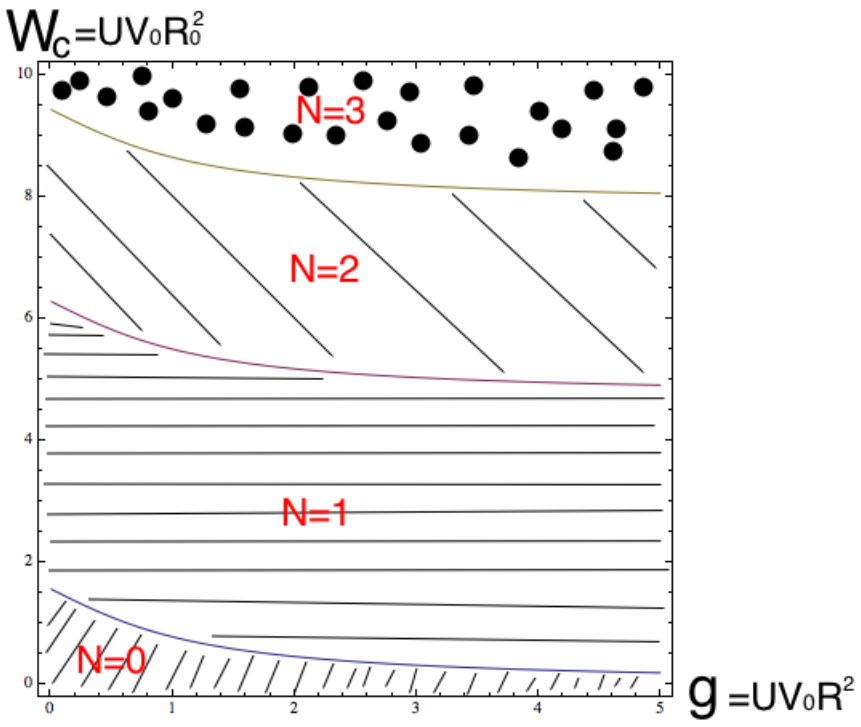

Figure 5.1: The critical curves of the spherical potential shell for $N = 1$, $N = 2$, and $N = 3$. These curves are obtained from Eq.(3.100) with $\mathbf{G_{shell}} = 0, \pi, 2\pi$, which indicate the critical curves of $N = 1$, $N = 2$, and $N = 3$ respectively.

5.1.3 Critical conditions

The critical condition is the only criterion which does not appear in both the $1D$ and $2D$ SE. The critical conditions only appear in $3D$ or higher dimensions of the SE. However, we find that the expanded Schwinger bound Eq.(3.13) gives with very high accuracy both the critical point and curve. Its prediction is valid to very high precision if we consider a high value of (n) in the kernel equation Eq.(3.13). We have defined the critical curve in two representations g and f. These representations are just to show the critical curve see Eqs.(3.102, 3.123). We found that the g repersentation gives us two points in the y and x axes. These two points represent the critical point of two potentials. For example, in the cutoff triangular potential Figure 3.11, the y-axis gives the critical point of the finite spherical potential, and the x-axis gives the critical point of the triangular potential. Also, we have defined the f-rep just because it is easier to compare with the estimating methods (for example see Figure 3.12).

If we have a potential with four or more parameters, we can define the critical surface in a number of dimensions equal to the number of parameters. However, potentials with more than three parameters are less common than potentials with a lower number of parameters.

5.1.4 Infinite versus finite number of bound state energies

We have studied this criterion in Ch.4. We have studied three potentials with a cutoff in order to investigate this criterion, and without the cutoff they have this expression

$$V(r) = -\frac{A}{r^m}, \tag{5.6}$$

where m and A are positive real numbers $m > 0$ and $A > 0$. If we do not use a cutoff for the potential with the form of Eq.(5.6), we will find zero or an infinite NBSE. We are confident about this since we found that all the estimating methods worked very well with our three choices $m = 1$, $m = 2$, and $m = 3$ in the fourth chapter. Therefore, according to the estimating methods utilized, potentials with a form of Eq.(5.6), always have an infinite NBSE or zero in some cases when $m = 2$. Then, when we include a cutoff near the origin, we find for $m = 1$ (the Coulomb potential) that this cutoff has no effect in terms of the infinite NBSE, which means this potential has an infinite NBSE before and after we perform the cutoff. In other words, as the cutoff is imposed on the Coulomb potential, all bound states of the pure Coulomb potential remain bound. Then, for the case $m = 2$, we also will get an infinite NBSE, just if $UA > 0.25$ in Eq.(4.76), and zero NBSE, if $UA < 0.25$. For $m = 3$ potential, when we performed a cutoff, we obtained a finite NBSE with a critical point. Thereafter, we can generalize this statement to include all positive real values of m in Eq.(5.6) by using the estimating methods. The following points summarize the observations:

1- If we do not have a cutoff, we always find an infinite NBSE, or zero when $m = 2$, and $AU > 0.25$.

2- If we perform a cutoff at the origin, if $m > 2$, it has a finite NBSE, if $m < 2$, it has an infinite NBSE, and if $m = 2$, it has an infinite or zero NBSE, depending on the value of UA.

3- If we perform the cutoff at $r = R_c$ as

$$V(r) = \begin{cases} -\frac{A}{r^m} & \text{if } 0 < r < R_c; \\ 0 & \text{otherwise,} \end{cases} \tag{5.7}$$

then, if $m > 2$,we find an infinite NBSE, and for $m < 2$, we obtain a finite NBSE. If $m = 2$ we find an infinite or zero NBSE.

We have found the previous points by using any one of the estimating methods explained in Ch.1. Therefore, for these potentials the infinite or finite NBSE depends on the location of the cutoff.

Then, in the fourth chapter, we found the critical point for the cutoff cubic inverse potential equals to 1.026 as in Eq.(4.88). Now, if we ask ourselves, what will happen to the critical point as we increase the power of the potential. In another words, let us assume that we have this potential

$$V(r) = \begin{cases} -\frac{A}{R_0^m} & \text{if } 0 < r < R_0; \\ -\frac{A}{r^m} & \text{otherwise.} \end{cases} \tag{5.8}$$

This potential is what we have studied in the fourth chapter. However, now we want to find the general behaviour of the critical point for $m > 2$. To do that we used the Brau-Calogero upper limit Eq.(3.17). By making $N = 1$ and calculating first term, we end up with

$$\mathbf{G_m^c} = \frac{AU}{R_0^{m-2}} > \frac{\pi^2(m-2)^2}{4m^2}, \tag{5.9}$$

where we have omit p and q in the B-C upper limit. Eq.(5.9) is graphed in Figure 5.2.

5.2 Future studies

Areas for future research include:

1- For a given potential, prove whether the FNE is same or not in all dimensions of SE? or is it same in the Dirac and the Klein-Gordon equation or not?

2- Extend this study to include the presence of an external effects such as the magnetic field or electric field.

3- Find new upper and lower limits of three or more particles to estimate the NBSE.

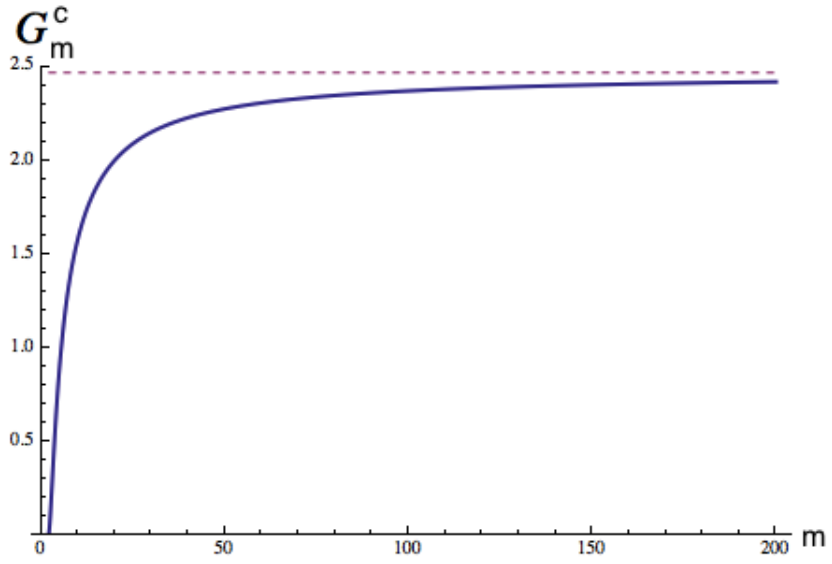

Figure 5.2: The critical points of the m inverse potential Eq.(5.8) for $m > 2$. As we can see when $m \to \infty$, the critical point goes to $\pi^2/4$ which is the critical point of the finite spherical point.

Bibliography

[1] Davisson, C.J. "The Diffraction of Electrons by a Crystal of Nickel". Bell System Tech. J. (USA: American Tel. and Tel.) **7**, 1, 90105 (1928). Retrieved December 5, 2012.

[2] N. Zettili, "Quantum mechanics concepts and applications", John Wiley & Sons, Inc, New York, **Ch.4**, 216-217 (2001).

[3] R. Jost and A. Pais, "On the scattering of a particle by a static potential", Phys. Rev. **82**, 840-851 (1951).

[4] V. Bargmann, "The spectrum of bound states in a central field of force", Proc. Nat. Acad. Sci. U.S.A. **38**, 961-966 (1952).

[5] F. Brau and F. Calogero, "Upper and lower limits on the number of bound states in a central potential", J. Phys. A: math. Gen. **36** (2003).

[6] F. Brau, "Sufficient conditions for the existence of bound states in a central potential", J. Phys. A, Math. Gen. **37**, 6687-6692 (2004).

[7] J. Schwinger, "On the bound states for a given potential", Proc. Nat. Acad. Sci. U.S.A. **47**, 122-129 (1961).

[8] C. Kocher, "Criteria for boundstate solutions in quantum mechanics", Am. J. Phys. **45**, 71-74 (1977).

[9] B. Simon, " The Bound State of Weakly Coupled Schrödinger Operators in One and Two Dimensions", Ann. phys. **97**, 279-288 (1976).

[10] K. Chadan, N. N. Khuri, A. Martin and T. T. Wu, "Bound states in one and two spatial dimensions", J. Math. Phys. **44**, 406-422 (2003).

[11] F. Brau, "Limits on the number of bound states and conditions for their existence", C. Benton "Studies in mathematical physics research", Nova Sci. Pub. **Ch.1**, 1-56 (2004).

[12] T. Aktosun, M. Klaus, and C. van der Mee, "On the number of bound states for the one-dimensional Schrödinger equation", J. Math. Phys. **39**, 4249-4256 (1998).

[13] K. Yang and M. de Liano, " Simple variational proof that any two dimensional potential well supports at least one bound state", Am. J. Phys. **3** 85-86 (1989).

[14] V. Glaser, H. Grosse, and A. Martin, "Bounds on the number of eigenvalues of the Schrödinger operator", Commun. Math. Phys. **59**, 197-212 (1978).

[15] K. Chadan, N. Khuri, A. Martin, Tai Tsun Wu, "Bound states in one and two spatial dimensions", J. math. phys. **44**, 406-422 (2003).

[16] R. G. Newton, "Bounds on the number of bound states for the Schrödinger equation in one and two dimensions", J. Operat. Theor. **10**, 119-125 (1983).

[17] F. Calogero, "Variable Phase Approach to Potential Scattering", Academic Press, New York, 1967.

[18] K. Chadan, "The asymptotic behavior of the number of bound states of a given potential in the limit of large coupling", Nuovo Cimento **A58**, 191-204 (1968).

[19] A. Martin, "Bound states in the strong coupling limit", Helv. Phys. Acta **45**, 140-148 (1972).

[20] F. Calogero, "Upper and lower limits for the number of bound states in a given central potential", Commun. Math. Phys. **1**, 80-88 (1965).

[21] J. H. E. Cohn, "On the number of negative eigenvalues of a singular boundary value problem", J. London Math. Soc. **40**, 523-525 (1965).

[22] V. Glaser, H. Grosse, A. Martin and W. Thirring, "A family of optimal conditions for the absence of bound states in a potential", in studies in mathematical physics- Essays in honor of Valentine Bargmann, edited by E. H. Lieb, B. Simon and A. S. Wightman, Princeton University Press, 1976, pp. 169-194.

[23] A. Martin, "An inequality on S wave bound states, with correct coupling constant dependence", Commun. Math. Phys. **59**, 293-298 (1977).

[24] K. Chadan, A. Martin, and J. Stubbe, "New bounds on the number of bound states for Schrördinger operators", Lett. Math. Phys. **35**, 213-219 (1995).

[25] F. Brau and F. Calogero, "Upper and lower limits for the number of S-wave bound states in an attractive potential", J. Math. Phys. **44**, 1554-1575 (2003).

[26] M. Cwickel, "Weak type estimates for singular values and the number of bound states of Schrödinger operators", Ann. Math. **106**, 93-100 (1977).

[27] S. Birman, "The spectrum of singular boundary problems", Math. Sb. **55**, 124-174 (1961), Am. Math. Soc. Transl. **53**, 23-80 (1966).

[28] R. Shankar, "Principles of Quantum Mechanics", Springer, Second Edition, **Ch.12**, 341-342 (1994).

[29] F. Marsiglio, "The harmonic oscillator in quantum mechanics: A third way", Am. J. Phys. **77**, 253-258 (2009).

[30] B. A. Jugdutt and F. Marsiglio, "Solving for three-dimensional central potentials using numerical matrix methods", Am. J. Phys. **81**, 343-350 (2013).

[31] V. Jelic and F. Marsiglio, "The double-well potential in quantum mechanics: a simple, numerically exact formulation", Eur. J. Phys. **33**, 1651-1666 (2012).

[32] F. Brau and F. Calogero, "Upper and lower limits for the number of S-wave bound states in an attractive potential", J. Phys. **44**, 1554-1575 (2003).

[33] Abramowitz, Milton Stegun, Irene A. "Handbook of Mathematical Functions with Formulas, Graphs, and Mathematical Tables", New York: Dover, **Ch. 10**, p. 446 (1965).

[34] A. A. Othman, M. De Montigny, F. C. Khanna, "Galilean Covariant Dirac Equation With a Woods Saxon Potential", Int. J. of Mod. Phys. E. **22**, (2013).

[35] M. Hamzavi, M. Movahedi, K. E. Thylwe, A. A. Rajabi. "Approximate analytical solution of the Yukawa potential with arbitrary angular momenta", Chinese Phys. Lett. **29**, (2012).

[36] E. R. Vrscay, "Hydogen atom with a Yukawa potential: Perturbation theory and continued-fractions-Padé approximants at large order", Phys. Rev. A **33**, 1433-1436 (1986).

[37] V. H. Badalov, H. I. Ahmadov and A. I. Ahmadov, " Analytical Solutions of the Schrodinger Equation with the WoodsSaxon Potential for Arbitrary l State", Int. J. Mod. Phys. E **18**, 631 (2009).

[38] Siegfried Flügge, "Practical Quantum Mechanics", Springer, Berlin, **Prob. 64**, 162-166 (1974).

[39] Erwin Schrödinger, "Collected Papers on Wave Mechanics", Published November 12th 2003 by American Mathematical Society (first published 1978).

[40] Albert Messiah, "Quantum Mechanics", North Holland Publishing Company (1967).

[41] L.D. Landau and E.M. Lifshitz, "Quantum Mechanics" (Volume 3 of A Course of Theoretical Physics) Pergamon Press 1965.

[42] P.M. Morse and H. Feshbach "Methods of Theoretical Physics", McGraw-Hill Book Company, Inc.; First Edition edition (1953).

[43] Konrad Jörgens, "Linear integral operators", Pitman, Boston, (1982),